Postprint of: Litwin W., Wasilczuk M., Wodtke M., Olszewski A., The influence of polymer bearing material and lubricating grooves layout on wear of journal bearings lubricated with contaminated water, TRIBOLOGY INTERNATIONAL Vol. 179 (2022), 108159, DOI: 10.1016/j.triboint.2022.108159

The influence of polymer bearing material and lubricating grooves layout on wear of journal bearings lubricated with contaminated water

Wojciech Litwin, Michał Wasilczuk[1], Michał Wodtke, Artur Olszewski

Gdansk University of Technology
Faculty of Mechanical Engineering and Ship Technology
ul. Narutowicza 11/12
80-233 Gdańsk, Poland

Abstract

The goal of the present paper is to investigate wear properties of journal sliding bearing operating in the conditions of contaminated water lubrication. Several bearing materials and bearing sleeve designs (differing in the axial grooves position and their shape) were tested experimentally under typical operating conditions in a dedicated test rig, which was equipped with a lubricating system, enabling lubrication with contaminated water. Results of the tests show that water contamination has a strong impact on the wear of the bearing system elements. It was revealed that some of the tested materials are beneficial in such demanding conditions and demonstrate lower wear rates. The design of the bearing bush also seems to have an impact on the wear, because bearings of different designs made from the same material demonstrated differences exceeding 100%. Higher water velocity in the lubricating grooves helps to minimize the wear of the stainless steel shaft. This was also confirmed by numerical simulations.

Keywords

polymer sliding bearings, water lubrication, hard particles, experimental testing

1 Introduction

The conditions for the generation of full film lubrication in sliding bearings are commonly known and result directly from solution of the Reynolds equation. However, in practice the operation of hydrodynamic bearings depends on many design and operational factors. One of them is the lubricant condition. It is common to assume that the lubricating fluid is free from contamination. However, this assumption is usually not true, even for new lubricating oils, the presence of a certain number of contaminant particles is allowed, depending on the specific requirements for particular applications [1]. The increased amount of contaminants in the lubricant may result from wear of the friction

[1] corresponding author, email: michal.wasilczuk@pg.edu.pl

surfaces, failure, and ineffectiveness of the seal or natural conditions, such as in the case of marine bearings or hydropower turbine bearings lubricated with unfiltered water from the environment. Hard particles getting into the lubrication gap of the hydrodynamic bearing damage or wear its sliding surfaces. The unfavorable influence of contaminants in the oil is usually limited by the use of bearing alloys, such as Babbitt alloys, one of the tasks of which is to allow the embodiment of solid particles [2]. Oil lubricated bearings are also used in shipbuilding, mainly because of their high durability and the absence of shaft corrosion [3]. However, this is a costly and complex solution due to the need to use reliable seals against oil leakages, while even small oil leakages of oil can be dangerous to the environment.

The influence of an increased amount of contaminants in the lubricating fluid on the operation of hydrodynamic bearings has been the subject of research for many years. Early experimental work concerned mainly oil-lubricated journal bearings [4–11] and was supplemented by theoretical studies of selected aspects of the influence of pollutants on the operation of hydrodynamic bearings [12–17]. For the purpose of experimental studies, various types of pollutants were introduced into the lubrication system (diatomaceous earth, steel machining chips, weld spatter, flyash, Al_2O_3, Air Cleaner Fine Test Dust, iron or quartz - SiO_2 particles, ISO Medium Test Dust) with a weight concentration of 0.0012% [10] up to 1.0% [4]. In other researches larger size contaminants were added, i.e., steel machining chips (a few to a dozen or so particles) or weld spatter [5]). The particles varied in size - from 1 μm [4] to even 1.4 mm [5]). The test results confirmed the negative impact of the presence of impurities in the oil on the bearing's performance, including an increase in resistance to motion (depending on the concentration of particles in oil [10, 12]), an increase in operating temperature [11] and increased surface wear. It has been proved that the wear mechanism depends on the particle size (mainly the possibility of their getting into the lubricating film [5, 11]) and their hardness. For example, the results from Vikström, et al. [9] indicate that hard Al_2O_3 particles can cause intensive abrasive wear to the bearing surface, while impurities with lower hardness (i.e., iron particles) result in much less wear in the form of polishing without the risk of failure. The wear of sliding surfaces also depends on their hardness and the hardness of dirt particles in the oil [6–8]. According to the work by Xuan et al. [8], the shaft wear is the lowest when it is much harder than the bearing surface or when its hardness is close to or greater than that of the particles. Khonsari et al. [13–15] investigated the influence of contamination on the occurrence of the phenomenon of scuffing, a wear process that involves a local increase in surface temperature above the critical temperature (flash temperature) at which the oil loses its protective properties, which causes the loss of the boundary layer and surface failure. Bou-Said et al. [16, 17] determined theoretically the operating parameters of a bearing lubricated with the lubricant in which rheological properties are changed due to the presence of impurities, assuming significant contents of particles in the oil (10-30 wt.%). The experimental results of the influence of

contaminants in the oil on the performance of hydrodynamic bearings (summarized synthetically in [18]) became the basis for determining the requirements of oil filtration for the safe operation of hydrodynamic bearings [11, 19]. A separate demand raised in the research was a bearing structure that would minimize the negative effects of the presence of contaminants. Dadouche et al. [20] examined bearings with surface texture and Sep et al. [21–23] bearings with a special helical groove machined on the shaft. The results of these works indicated that it is possible to reduce the surface wear caused by particles in the oil compared to cylindrical bearings by changing the design of the bearing.

Recently, due to the growing importance of environmental protection, intensive research has been carried out on the feasibility of replacing lubricants that are potentially dangerous to the environment with other ecological liquids. More environmentally friendly lubricants based on water, esters, glycols, etc. (so-called EAL - environmentally acceptable lubricants) are used. It is possible to replace mineral oil with an environmentally friendly lubricant without the need to modernize bearings with whitemetal bushings [24]. Water-lubricated bearings are also developed, operating in a closed circuit system, where filtered fresh water is circulating in the sealed system, or in an open system, when the surrounding water serves as a bearing lubricant [25, 26].

In the case of bearings operating in open systems (e.g., stern tube bearings of propeller shafts, guide bearings of water turbines), the presence of contaminants that occur naturally in water is inevitable [27–29]. General conclusions about the influence of contamination on the performance of oil-lubricated hydrodynamic bearings can, according to the authors, be correlated to water-lubricated bearings only to a limited extent. Both lubricants differ significantly in physical parameters and lubricity and the materials from which the bearings are made are different. In the case of water-lubricated bearings, NBR rubber is often used, one of the advantages of which is greater tolerance to lubrication with contaminated liquid, as compared to lignum vitae [30]. Other materials, such as polymers or sintered brass [26,31] are also used. It is worth noting that the existing practical recommendations for water-lubricated bearing materials do not consider the problem of operation with contaminated lubricant [32].

The literature provides extensive results of tribological tests of materials used for water bearings carried out under contaminated lubrication conditions. Most often, sediments obtained from the natural environment were used for the research, e.g., Yangtze River [29, 33, 34] or the Gulf of Mexico Coast [35, 36], but also, for example, Al_2O_3 [37] or quartz particles [34]. The average particle size distribution of the impurities was usually in the range from a few to a maximum of 300 μm. Tribological tests of NBR rubber in the conditions of lubrication with contaminated water with a concentration of 1.1 wt. % were carried out [29, 34]. The results indicated a strong dependence of the wear and friction coefficient on the concentration and size of the particles. Solid particles in water destroyed the

lubricating film causing abrasive wear. At the same time, no traces of transfer of the rubber material to the mating surfaces (stainless steel, brass) were found. Yang et al. [34] performed a comparative study of the impact of the type of impurity on NBR wear. The obtained results indicated that material wear as a result of SiO_2 particles of a given size was greater than that in the case when the natural sediments of the same grain size also contained clay in addition to SiO_2. In the case of polymeric materials, tribological tests under the conditions of water lubrication with contaminants were aimed, among others, at investigating the effect of filler contents and polymer hardness on their wear rate [38, 39].

All the tribological tests of NBR and polymers described above were carried out on tribometers and not on the bush-shaft arrangement as in the journal bearing. For this reason, the test conditions reproduced the bearing operating conditions only to a limited extent, because the configuration of the contact was different, and thus the transport of pollutants in the film. In order to fully take into account the operating conditions of the bearing, it is necessary to conduct experimental tests on real objects, which requires special test stands [40] and the results of such works available in the literature are sparse [41].

The main goal of the present research was to investigate the effect of the material and the polymer sleeve design on the intensity of wear of journal bearing systems lubricated with contaminated water. Due to the complexity of the phenomena taking place in operation with contaminated lubricant it was decided to test bearing models similar to the real polymer bearings. Three materials and four designs of the bearing (differing mainly with the number, shape, and arrangement of axial lubricating grooves) were tested experimentally under typical operating conditions of water lubricated bearings (in terms of the sliding speed and specific load) in order to find the influence of polymer bearing material and bearing design on the intensity of wear of both, polymer bearing bush and the steel shaft. Experimental investigations, containing a series of long duration tests, were carried out on the specialized test stand equipped with a separate lubricating system, enabling lubrication with the contaminated water.

Experimental investigations were supplemented with CFD (*Computational Fluid Dynamics*) calculations of the water flow in selected bearing designs. The goal of the theoretical research was to investigate the effect of the bearing geometry on the water streamlines and thus on the potential trajectory of the solid particles dispersed in the lubricant (which is mainly driven by water flow).

2 Materials and Methods

2.1 Test stand

Experimental tests were carried out on the hydrodynamic journal bearing test stand allowing for long-term tests under lubrication with contaminated water (Fig. 1). In order to provide a homogeneous

distribution of the contaminating sand particles (mainly SiO_2), two tanks with mixers were used together with a peristaltic pump supplying contaminated water directly to the test bearing housing, which is shown in a schematic view (Fig. 1 b). Lubricating water was then passing axially through the grooves in the bearing bush and to the lubricant tank, in a similar manner as in a real ship or water turbine (see the cross-section of the test head - Fig. 1 c). An excess of the lubricating water was returning to the system via an outflow. Test bearing was loaded by a hydraulic piston pressing the shaft via a roller element bearing (shown in Fig. 1 b). The housing design provided the ability to tilt, which prevented edge loading of the bearing bushes. Test shafts were designed as exchangeable stainless steel sleeves to test a new set of a bearing sleeve and a shaft each time.

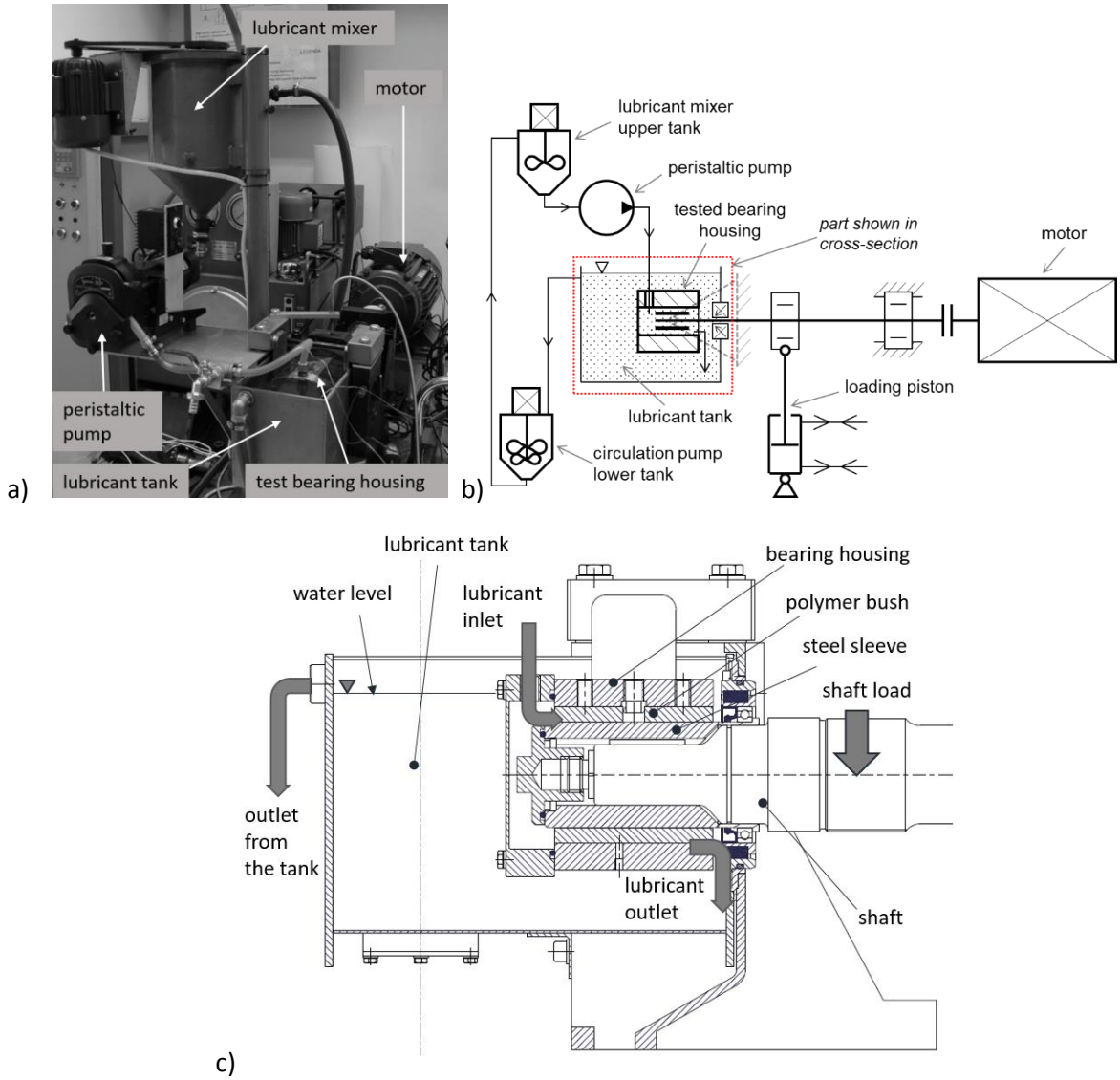

Fig. 1. Test stand; a) general view, b) schematic view, c) test head cross-section.

2.2 Tested bearings

Four designs of bearing sleeves (originated from real bearing applications) were tested. Test sleeves differ in the shape and number of open axial grooves (as shown in Fig. 2):

- Bearing with two cylindrical grooves,
- Bearing with six rectangular grooves in the upper half of the bearing and chamfered groove edges (1x45°),
- Bearing with six rectangular grooves in the upper half of the bearing and sharp groove edges,
- Bearing with six rectangular grooves with wider spacing of grooves, including two at the lower half of the bearing.

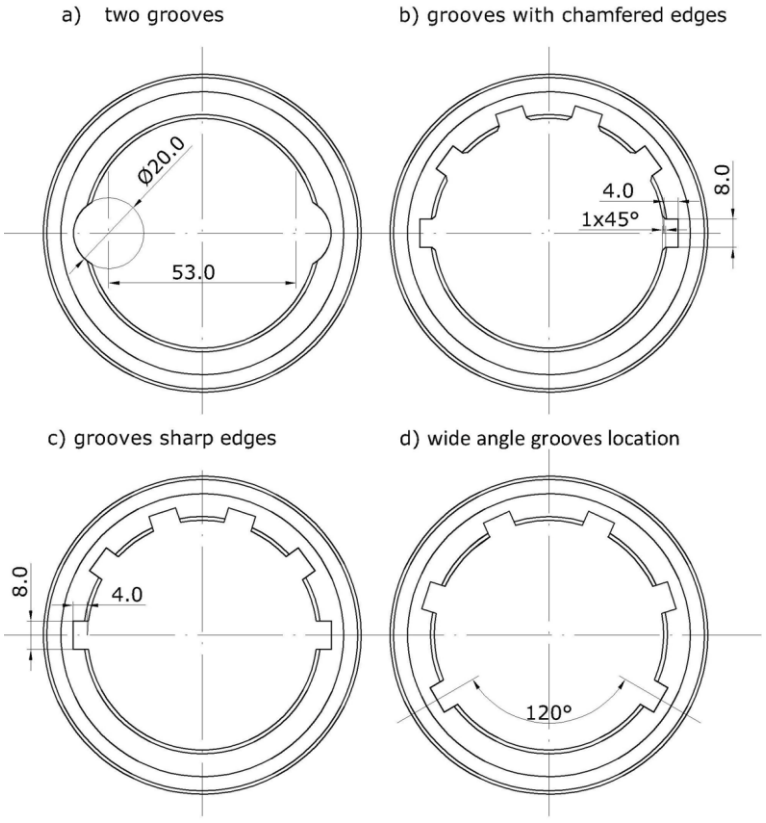

a)

Fig. 2. Test bearings a) two grooves, b) upper half grooves with chamfered edges, c) upper half grooves with sharp edges, d) wider spacing of the grooves.

There are no clear recommendations concerning certain applications of the presented bearing geometries and various manufacturers, according to their own experience, use different layout of the lubricating grooves, as well as the chamfered or sharp edge of the groove, as shown respectively in Fig 3 a and b.

It is not known how the chamfers vs. sharp edges of the groove influence the wear of the bearing system lubricated with a contaminated fluid. It seems, that in the case of chamfered grooves solid particles can enter the film more easily, due to the converged wedge in the entry zone, while sharp

edges will prevent the solid particles from entering the film, but these speculations are not supported by any research results, theoretical or experimental known to the authors.

a)  b) 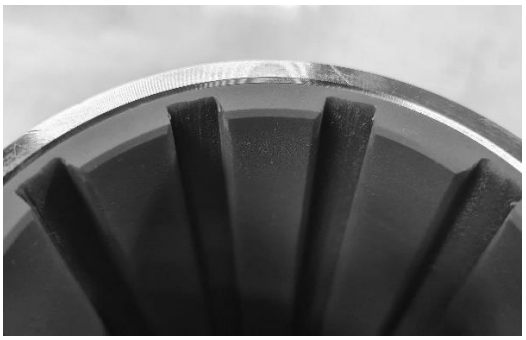

Fig. 3. Two styles of the lubricating groove edges a) sharp edges, b) chamfered edges.

The bush with each groove design (four different geometries, as shown in Fig. 2) was made from three different types of commercially available bearing materials:

- polymer material (marked as A),
- three layer composite material with rubber layer lined with filled PTFE (marked as B),
- composite material based on a special synthetic fabric impregnated with a thermo-setting resin (marked as C).

The main characteristics of the bearing sleeve materials are collected in Table 1, hardness of the polymer materials is not given in manufacturers' data. The exchangeable journals were made of austenitic stainless steel X10CrNi18-8, equivalent to AISI 301 with the hardness of 25-26 HRC, machined to approximately Ra0.5 roughness. Chemical composition of steel sleeve is given in Table 2,

Table 1. Bearings material data.

Material type	Modulus of elasticity [MPa]	Water swell [%]	Thermal expansion coefficient x 10-5 [1/K]
thermoplastic polymer (A)	610	1.6	20
3 layers composite(B) (PTFE/NBR/bronze)	770 / 40 / 103 000	0 / 0 / 0	12.4 / 17 / 2.2
thermoset polymer with fibers (C)	2800	0.5	5 - 10 (depending on direction)

Table 2. Chemical composition (wt%) of stainless steel journal.

C	Si	Mn	Ni	P	S	Cr	Mo	N
0.05 - 0.15	max 2	max 2	6 - 9.5	max 0.045	max 0.015	16 - 19	max 0.8	max 0.11

2.3 Experimental procedure

Additionally to a problem of lack of standards for testing bearings lubricated with contaminated fluid, there is also an ambiguity of type and quantity of hard particles dispersed in a lubricating water for tests. The authors collected samples of water from a small river after a heavy rainfall. Analysis of the amount of contaminating solid particles showed that their concentration could be as large as 5 cm³ / liter.On one hand this was the amount practically occurring in natural conditions, on the other hand this amount caused quite fast wear of the polymer bushes, as the pilot tests showed. Tests conditions and details of lubricating water finally used in the research are collected in Table 3.

Table 3. Bearings tests conditions and details of applied lubricating medium (contaminated water).

Load (specific load)	Speed	Water flow	Particles concentration	Volume of solid particles	Water volume in the system
4480 N (0.65 MPa)	430 rpm	3 l/min	0.5 ‰	5 cm^3/liter	10 liters

The contaminant is mainly composed of SiO_2 particles. Examples of the particle size distribution and the microscopic photo of the particles is shown in Fig. 4. Microscopic images show that the grains are rounded, without sharp edges, which is typical of sedimentary material carried by rivers.

Water with solid particles was in constant motion in the system, due to stirring in a lubricant mixer, to prevent sedimentation of particles. The total time of one wear test was 70 hours of operation including the running-in phase (Table 4). Sliding distance under lubrication with contaminated water was equivalent to approximately 315 000 m. During each test, the lubricating water was changed four times (every 15 hours of operation) in order to introduce a new quantity of solid particles, which during the operation were constantly degraded as a result of wear.

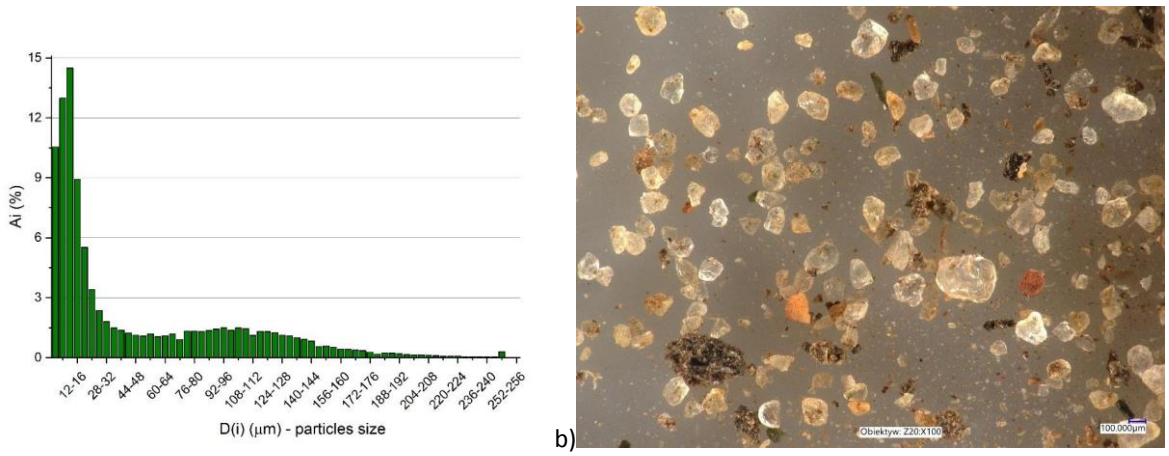

a) b)

Fig. 4. Solid particles added as water contamination; a) example of particles size distribution in one portion of contamination, b) microscopic view (x100).

Table 4. Testing procedure.

#	Description	Duration	Comment
1	Running-in stage	10 h	two phases (each 5h long); speed 260 and 430 rpm; load 4480 N (0.65 MPa) water without particles
2	Wear test stage	60 h	four phases (each 15h long); speed 430 rpm; load 4480 N (0.65 MPa) fresh lubricating medium with solid particles in each phase

Linear wear of the bearing sleeves was evaluated by wall thickness measurements before and after the test, in three cross sections – one vertical, in line with the load, and two other in the cross sections 15° apart (Fig. 5).

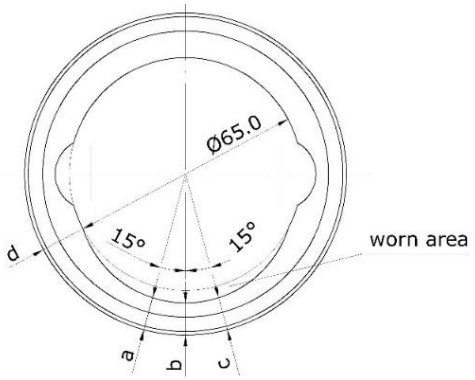

Fig. 5. Schematic of the bearing sleeve wear measurements.

Measurements were done in front and in the back of the bearing sleeve before and after the wear test. Wear in each location was evaluated as the difference between the thickness of the bush before and after the tests. Representative linear wear of the bearing sleeve shown in the paper was calculated as an average of wear in six positions, where appropriate the graphs with the results show the standard deviation of the evaluated wear. The condition of the steel shaft was also checked - the surface profile of the shaft was measured in the axial direction, with the use of a profilometer which allowed us to evaluate its linear wear (with the use of Jenoptik Hommel Etamic T8000 contact profilometer). In this way the wear of both polymer bearing sleeves and steel shafts were evaluated, as well as the changes in the roughness of the steel shafts. Finally, the program of the experimental tests covered five bearings sleeves made of each material: four designs (as shown in Fig. 2) lubricated with contaminated water, and the sleeve with two grooves (Fig. 2a) was additionally tested under water lubrication without contaminants. This allowed assessing the influence of the presence of solid particles in the lubricating water on bearing wear.

3 Results and discussion

3.1 Effect of contamination

A comparison of the measured linear wear of the bearing sleeve and steel shaft for clean and contaminated water lubrication is shown in Fig. 6. It was tested with the use of the bearing bushes with two cylindrical grooves (style a) made from each of three materials. The results revealed that, as far as sleeve wear is concerned, there is a predominant influence of the material. Material A demonstrates wear (maximum measured wear ~165 µm), which is an order of magnitude larger than that of material B and more than two times larger than that of material C. The influence of the cleanliness of the lubricant is significant but smaller than the effect of the material. The assessed linear wear of the shafts was significantly smaller in comparison to bearing sleeves wear (maximum measured value ~5 µm). On the other hand, wear of the steel shafts seems to be much less affected by the bush material type, than by the water contamination.

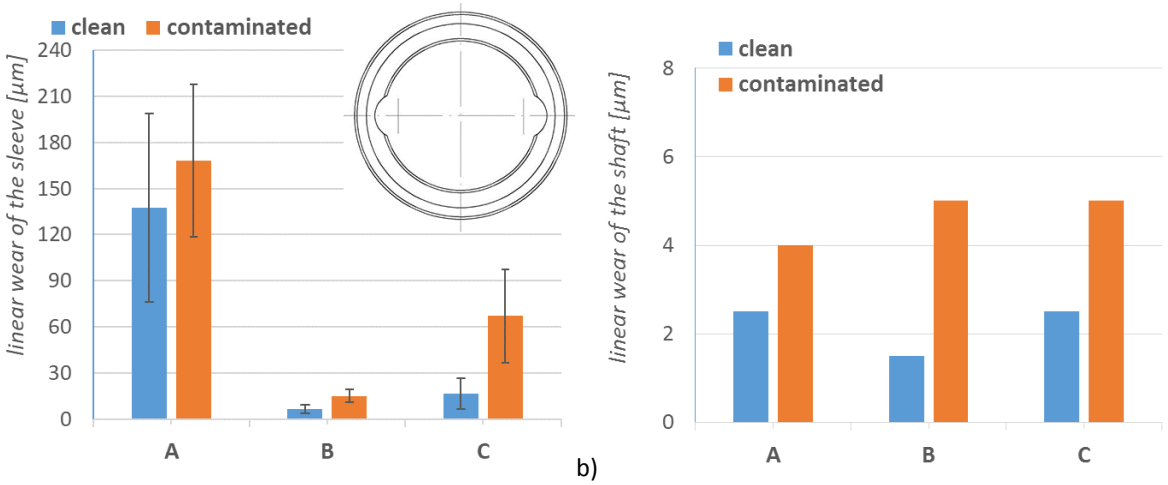

Fig. 6. Comparison of the linear wear a) of the bearing sleeve – with standard deviation bars, and b) the steel shaft, lubricated with clean and contaminated water for different materials (A, B, C) and two cylindrical grooves geometry (style a).

In Fig. 7 photographs of the sleeves after tests are shown for all tested materials. One can see different patterns of wear between the various materials, with quite heavy wear of material A. Wear of bushes in clean and contaminated water does not differ significantly but the angular extent is slightly larger for contaminated water lubrication. In all cases, worn areas are smoother than the bush surface outside the wear area. This was also confirmed by the roughness measurements after the tests.

a)

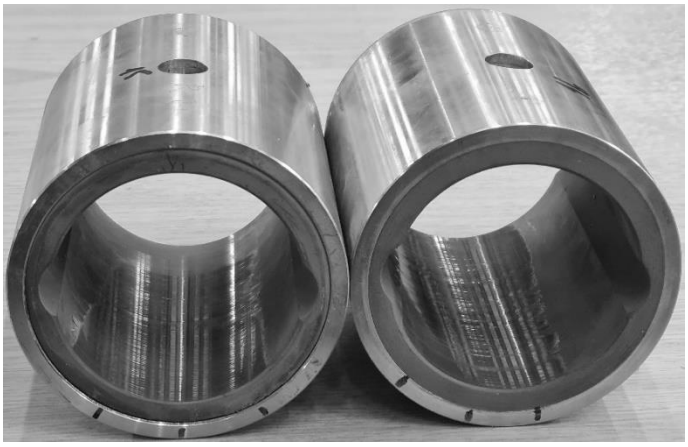

b)

c)

Fig. 7. Photographs of the bearing sleeves after tests lubricated with clean water (left-hand side) and with contaminated water (right-hand side): a) made of polymer (material A), b) 3 layers type (material B), c) made of thermoset composite (material C).

The wear process has also a significant effect on components' surface roughness parameters, which is shown in Fig. 8. For both lubricant conditions, clean and contaminated, the polymer bush roughness parameter is significantly decreased during the test. The result differs much for the steel shaft roughness (Fig. 8 b), its roughness remains almost unchanged when it is lubricated with clean water (except for the shaft rubbing against material C), while the roughness increases when the shaft is

lubricated with the contaminated water, by 20% (for material C) to approximately 50% (for materials A and B).

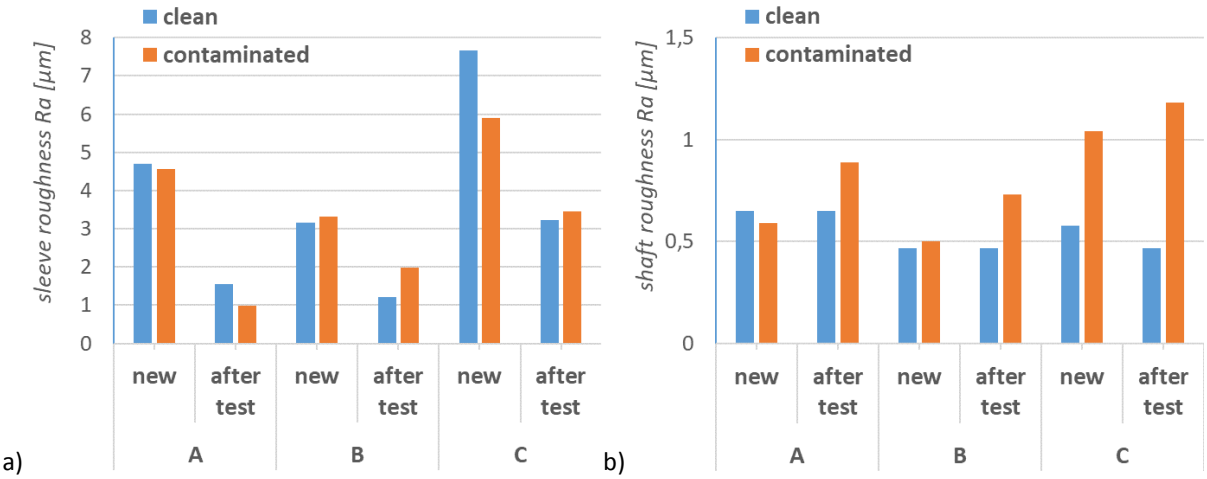

Fig. 8. Roughness Ra parameter measured before and after the tests in clean and contaminated water; a) bushes, b) shafts.

Images of the worn shaft are presented in Fig. 9, after the test in clean and contaminated water lubrication, one can observe more circumferential scratches after lubrication with contaminated water.

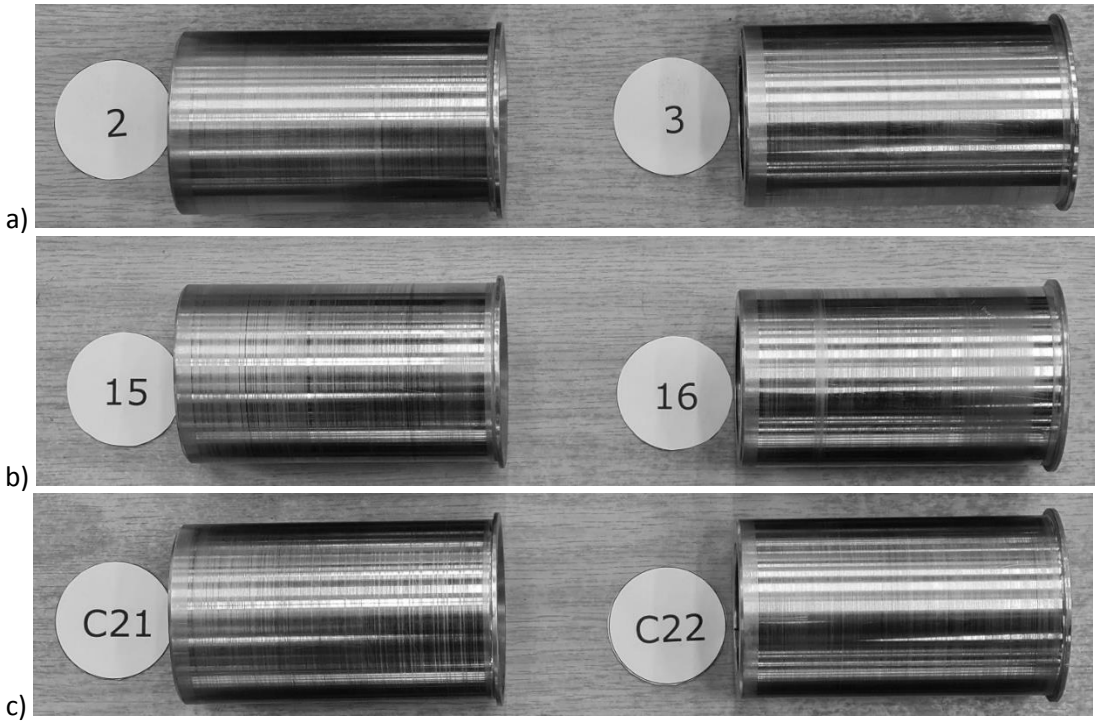

Fig. 9. Pictures of the shaft after tests with clean (left-hand side) and contaminated water lubrication (right-hand side); a) tested with sleeve A, b) tested with sleeve B, c) tested with sleeve C.

3.2 Effect of bearing sleeve geometry

Fig. 10 a) shows the linear wear of the polymer bearing sleeves made of the tested materials (A, B, and C) in various geometrical configurations (a, b, c, d). It can be noticed that the influence of the type of material is more pronounced than the influence of the sleeve geometry. Polymer material A has a linear wear almost an order of magnitude greater than the other tested materials, with the multi-layer material B has a slightly smaller wear than the composite material C. The influence of the configuration of the lubricating grooves is also visible, especially for polymer material A, but it is not so significant. The configuration with two cylindrical cross-section grooves seems to be only slightly more favorable than the others, this is noticeable for the two materials (A and B), whereas in the composite material C the influence of the configuration of the grooves is not very pronounced, with the wear in all configurations very close to one another. Macroscopic image of the worn areas confirms this finding, because the worn areas for each material look similarly in terms of smoothness and number of visible deep scratches, which can be observed on the surface. The wear is uniform along the bush axis.

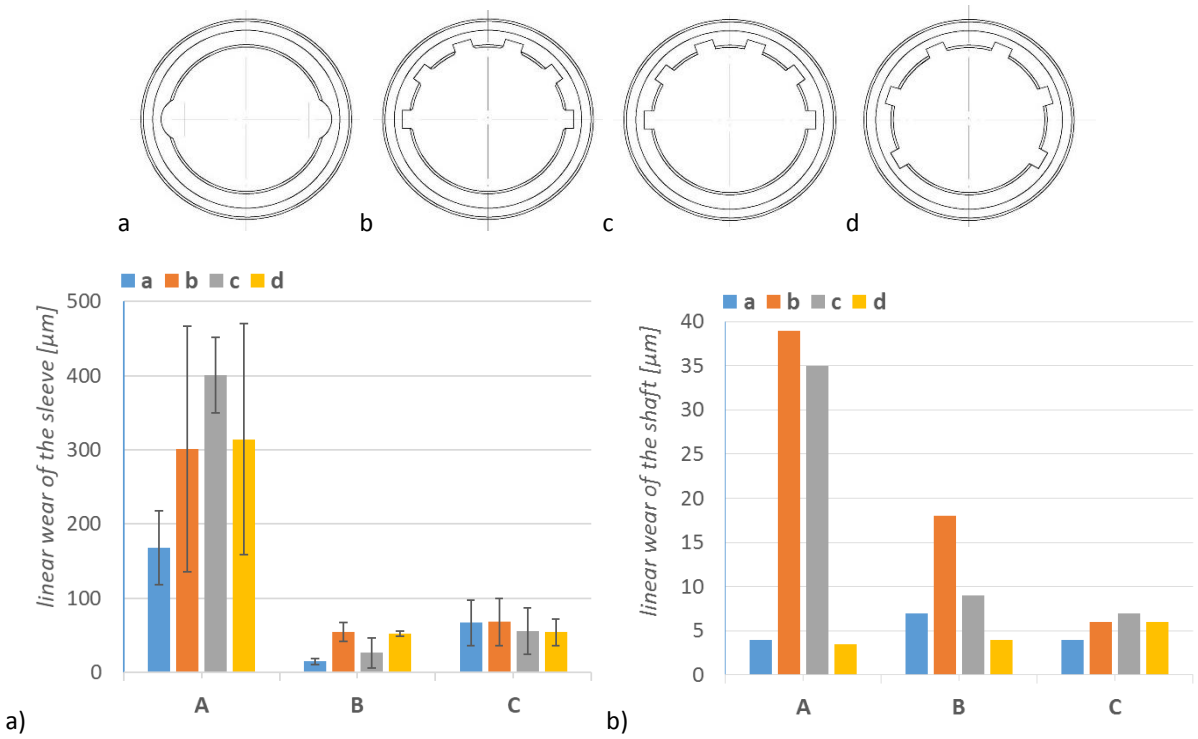

Fig. 10. Comparison of the linear wear: a) of the bearing sleeve – with standard deviation bars, and b) the steel shaft, both lubricated with contaminated water for different materials (A, B, C) and geometries of the sleeve (styles a, b, c, d).

Wear of the steel shaft is shown in Fig. 10 b), it is an order of magnitude smaller than that of the polymer bush, but in technical circumstances its wear is very important, because the shaft is usually much more difficult and costly to replace than the polymer bush. Looking at the worn surface of the shafts one can observe quite regular wear marks with some deeper scratches distributed randomly along the contact area. The linear wear of the steel shaft to some extent also depends on bush material, but the differences between shafts rubbing against the various materials are much smaller.

A larger influence of the lubricating grooves configuration can be observed, with cylindrical grooves (a) and the grooves with wider spacing (d) being the configurations yielding smaller wear in all three material cases, than these with sharp or chamfered edges of the grooves located only in the unloaded half of the bush (b and c). The style of the edge (sharp vs chamfer) does not seem to be a significant factor in all materials – sharp edges are considerably better for materials A and B, while in material C, an opposite, but much smaller difference is observed.

3.3 CFD analysis of lubricant flow in the bearing

In order to investigate the structure of the fluid flow in the bearing, and thus the potential influence of the internal geometry (shape and number of grooves) on the movement of contaminants carried with the lubricating water, numerical analyzes were performed using CFD (Computational Fluid Dynamics). It was assumed that the lubricating water flow was incompressible, turbulent (SST model) taking into account cavitation (Rayleigh-Plesset model). The calculations were made for two cases of bearing geometry: cylindrical grooves (style a) and six rectangular grooves with sharp edges (style c). Water flow was modeled in the gap, axial grooves, and in the inlet and outlet areas of the bearing gap (Fig. 11), with the following assumptions:

- viscosity of 0.001 [Pa s] at 20^{o}C,
- inlet with a flow rate of Q = 3 l / min,
- outlet with forced axial flow in the direction of the z-axis,
- the surface of the shaft rotated around the bearing axis with the angular velocity ω, with the condition of no slippage,
- all external walls of the model were assumed to be stationary with the condition of no slippage on the wall.

To obtain the appropriate quality of the elements, the computational mesh, depending on the analyzed case of bearing geometry, was divided into 2.3 to 2.6 million of finite volumes (12 divisions across the thickness of the film). Additional volumes at the inlet and outlet of the slot (25 mm axial length, 80 mm OD) allowed to move the boundary conditions (Inlet, Outlet) away from both ends of the lubrication gap and to calculate the desired water flow conditions at the edges of the slot and axial grooves. The dimensions of the bearing in the CFD calculations (diameter, length) and axial grooves were assumed the same as in the laboratory tests (see Fig. 2), the diametral clearance was 0.15 mm.
The use of CFD allows for the analysis of the bearing operation in the conditions of fluid film friction. For this reason, the calculations were carried out assuming that the minimum film thickness was 10 μm and selecting the bearing attitude angle in the course of iterative calculations so that the resultant

hydrodynamic force had a vertical direction (horizontal component <± 1 N), the shaft rotational speed in the calculations was 1000 rpm.

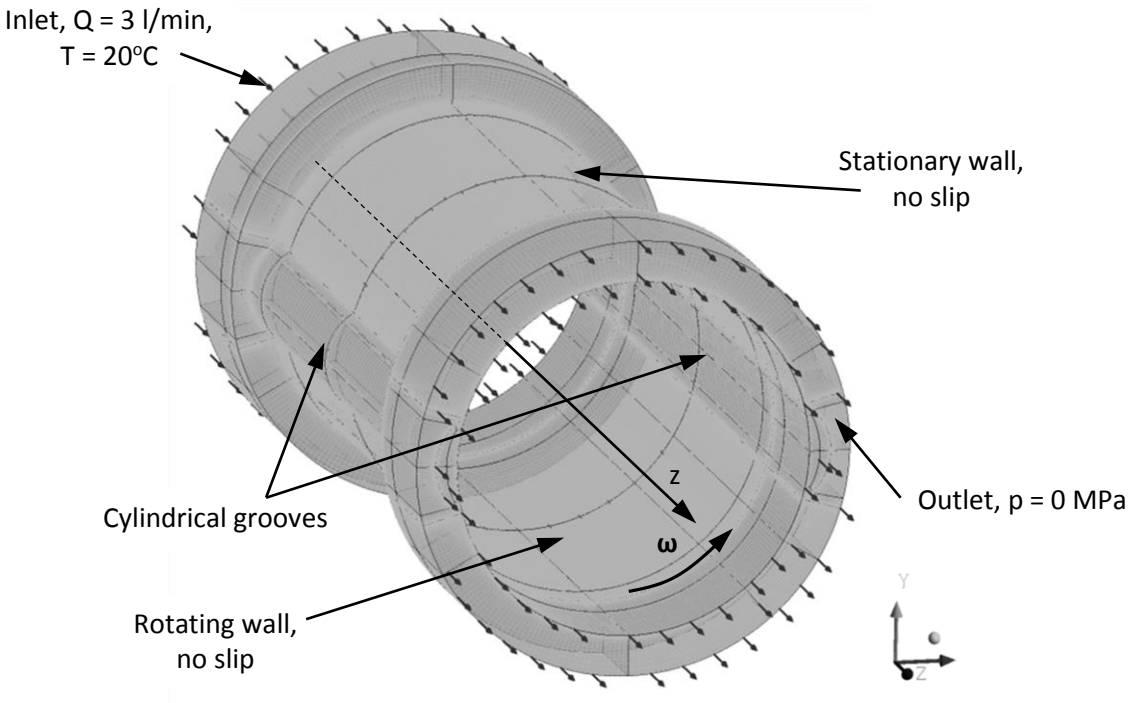

Fig. 11. Computational mesh for CFD calculations with marked boundary conditions – geometry with the cylindrical grooves.

Bearing load with these assumptions was much lower than the one applied in the experiments, nevertheless, the conclusions drawn from the results (flow pattern) are still valid, since, as confirmed with CFD calculations, water flow took place almost only through grooves.

Results of CFD calculations of the velocity streamlines and axial velocity profiles in groves on the selected axial cross sections of the bearing are shown respectively in Fig. 2 and Fig. .

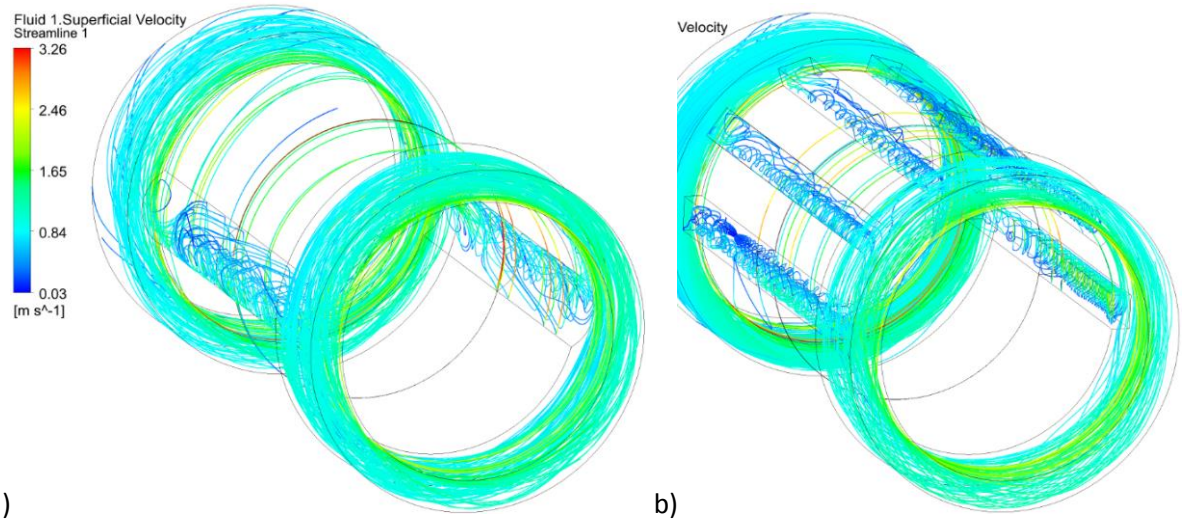

a) b)

Fig. 12. Streamlines of the lubricant, view from the outlet side a) cylindrical grooves, b) six rectangular grooves with sharp edges.

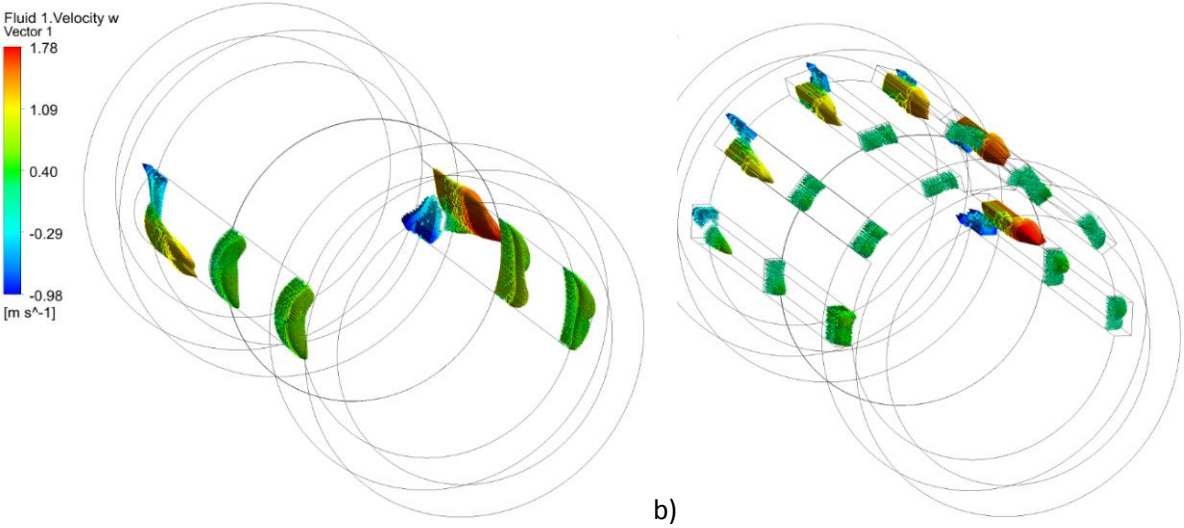

a) b)

Fig. 13. Axial velocity of the fluid in the grooves at three cross sections (inlet, mid-plane, outlet), view from the outlet side; a) cylindrical grooves, b) six rectangular grooves with sharp edges.

The calculated flow lines for the flow of water in the bearing reveal, in addition to the axial flow between the inlet and the outlet, a strong eddy flow inside the grooves due to the rotational movement of the shaft. Overall, it can be stated that the flow structure in the grooves is very complex. A similar picture was obtained both for the geometry of the bushings with cylindrical and rectangular grooves.

Analysis of the results of the axial velocity distribution in the grooves reveals that there are backflows in the inlet area and the flow becomes unidirectional over the entire cross-section of the grooves in the center and outlet areas of the bearing. The quantitative analysis of the obtained flow results is summarized in Table 5.

In the table, detailed values of the calculated flow rates and average axial velocities at the bearing mid-length cross-section were presented separately for each groove and water film section (TOP – thickest film zone and BOTTOM – thinnest film zone). The speed of the water in the grooves was used to analyze the potential of the flow to transport the contaminating particles.

Regardless of the analyzed geometry of the bearing, the axial flow of water takes place almost entirely through the grooves. Higher flow rates Q (and the closely related mean axial flow velocities Vz) were observed for the geometry with cylindrical grooves as compared to the geometry with rectangular grooves. This is caused by the fact that the cross-sectional area of the grooves is approximately two times smaller in cylindrical grooves, which results (for the same forced flow rate) in higher axial flow velocities. This is, most likely, the main circumstance that prevents contaminants carried by the lubricating water from getting into the fluid film. The higher flow velocity (kinetic energy) allows contaminants to be transported more efficiently between the bearing inlet and outlet.

Table 5. Results of CFD calculations of parameters of the bearings with different groove arrangements

			cylindrical grooves (geometry a)	rectangular groves with sharp edges (geometry c)
Angular position of minimum film thickness Kąt h_{min} - γ		deg	310.7	313.2
Vertical load F_Y / mean pressure		N / MPa	572.2 / 0.084	542.9 / 0.079
Cross section of a single groove		mm^2	49.5	32
Total cross-section of all grooves		mm^2	99	192
water flow Q / average axial velocity V_z (at mid bearing length cross section)	Film TOP	l/min / m/s	0.003 / ~ 0	0.007 / ~ 0.02
	Film BOTTOM		~ 0 / ~ 0	~ 0 / ~ 0
	Groove 0°		1.688 / 0.56	0.549 / 0.28
	Groove 36°		-	0.554 / 0.28
	Groove 72°		-	0.448 / 0.22
	Groove 108°		-	0.458 / 0.23
	Groove 144°		-	0.525 / 0.26
	Groove 180°		1.309 / 0.42	0.459 / 0.23
	Total		~ 3 / -	~ 3 / -

4 Conclusions

The obtained results can be summarized as follows:

- Lubrication with water contaminated with hard particles is a frequently encountered regime of operation of marine and hydropower ecological bearings, but little literature data is published.
- Quite expectedly wear rate in contaminated water was larger, and the wear rate of the polymer sleeve bush and steel shaft increased by 40-300% and 30-400% respectively in comparison to clean water lubrication.
- In the contaminated water, bearing material choice had the largest influence on the wear rate of the bearing bush – various tested bearing materials demonstrated the wear rate differing by a factor of 3 to 8.
- The influence of the bearing design (the arrangement of the lubricating grooves) was also considerable – the differences between the bearings made from the same materials and differing by the design were over 100% in some cases – this finding necessitates the collection of component level testing data for reliable determination of wear rates of composite bearing materials
- In the case of steel shaft, the influence of bearing bush polymer material was less significant than the influence of groove design.
- The expected influence of chamfer vs. sharp edge of the grooves on wear rate was not consistently confirmed; and
- CFD calculations also show that the advantage of cylindrical grooves may be due to higher water velocity in the lubricating grooves, helping to wash out the contaminating particles.

5 Acknowledgments

This work was a part of research grant no. 2016/23/B/ST8/03104 entitled “Research on water-lubricated sliding couples in unfavorable operating conditions” financed by the Polish National Science Centre.

Computations were carried out using the computers of Centre of Informatics Tricity Academic Supercomputer & Network (TASK)

6 References

[1] D. Margaroni, Oil cleanliness, Lube-Tech. 25 (2002) 1–4. https://www.lube-media.com/lube-tech/.

[2] W.M. Hannon, M.J. Braun, Hydrodynamic Journal Bearings, Encycl. Tribol. (2013) 1736–1748. https://doi.org/10.1007/978-0-387-92897-5_41.

[3] W. Litwin, Experimental research on marine oil-lubricated stern tube bearing, Proc. Inst. Mech. Eng. Part J J. Eng. Tribol. (2019). https://doi.org/10.1177/1350650119846004.

[4] S.A. McKee, Effect of abrasive in lubricant, SAE Trans. (1927) 73–77.

https://doi.org/10.4271/270009.
[5] R.C. Elwell, Foreign Object Damage in Journal Bearings., Lubr. Eng. 34 (1978) 187–192.
[6] A. Ronen, S. Malkin, Wear mechanisms of statically loaded hydrodynamic bearings by contaminant abrasive particles, Wear. 68 (1981) 371–389. https://doi.org/10.1016/0043-1648(81)90183-6.
[7] A. Ronen, S. Malkin, Investigation of Friction and Wear of Dynamically Loaded Hydrodynamic Bearings With Abrasive Contaminants, J. Tribol. 4 (1983) 559–567.
[8] J.L. Xuan, I.T. Hong, E.C. Fitch, Hardness effect on three-body abrasive wear under fluid film lubrication, J. Tribol. 111 (1989) 35–40. https://doi.org/10.1115/1.3261876.
[9] V. Wikström, E. Höglund, R. Larsson, Wear of bearing liners at low speed rotation of shafts with contaminated oil, Wear. 162–164 (1993) 996–1001. https://doi.org/10.1016/0043-1648(93)90110-8.
[10] K. Mizuhara, M. Tomimoto, T. Yamamoto, Effect of particles on lubricated friction, Tribol. Trans. 43 (2000) 51–56. https://doi.org/10.1080/10402000008982312.
[11] J.K. Duchowski, K.G. Collins, W.M. Dmochowski, Experimental evaluation of filtration requirements for journal bearings operating under different contaminant levels, Lubr. Eng. 58 (2002) 34–39.
[12] M. Tomimoto, K. Mizuhara, T. Yamamoto, Effect of particles on lubricated friction - Theoretical analysis of friction caused by particles in journal bearing, S.A.E. Trans. 45 (2002) 47–54. https://doi.org/10.1080/10402000208982520.
[13] M.M. Khonsari, S.H. Wang, On the role of particulate contamination in scuffing failure, Wear. 137 (1990) 51–62. https://doi.org/10.1016/0043-1648(90)90017-5.
[14] M.M. Khonsari, M.D. Pascovici, B.V. ny Kucinschi, On the Scuffing Failure of Hydrodynamic Bearings in the Presence of an Abrasive Contaminant, 1 (1999) 90–96. https://doi.org/https://doi.org/10.1115/1.2833816.
[15] M.D. Pascovici, M.M. Khonsari, Scuffing failure of hydrodynamic bearings due to an abrasive contaminant partially penetrated in the bearing over-layer, J. Tribol. 123 (2001) 430–433. https://doi.org/10.1115/1.1329877.
[16] B. Bou-Said, H. Boucherit, M. Lahmar, On the influence of particle concentration in a lubricant and its rheological properties on the bearing behavior, Mech. Ind. 13 (2012) 111–121. https://doi.org/10.1051/meca/2012006.
[17] H. Boucherit, B. Bou-Saïd, M. Lahmar, The effect of solid particle lubricant contamination on the dynamic behavior of compliant journal bearings, Lubr. Sci. 29 (2017) 425–439. https://doi.org/10.1002/ls.1378.
[18] M.M. Khonsari, E.R. Booser, Effect of contamination on the performance of hydrodynamic bearings, Proc. Inst. Mech. Eng. Part J J. Eng. Tribol. 220 (2006) 419–428. https://doi.org/10.1243/13506501J00705.
[19] J.K. Duchowski, Examination of journal bearing filtration requirements, Lubr. Eng. 54 (1998) 18–28.
[20] A. Dadouche, M.J. Conlon, Operational performance of textured journal bearings lubricated with a contaminated fluid, Tribol. Int. 93 (2016) 377–389. https://doi.org/10.1016/j.triboint.2015.09.022.
[21] J. Sep, A. Kucaba-Pi, Experimental testing of journal bearings with two-component surface layer in the presence of an oil abrasive contaminant, Wear. 249 (2001) 1090–1095. https://doi.org/10.1016/S0043-1648(01)00848-1.
[22] J. Sep, L. Tomczewski, L. Galda, A. Dzierwa, The study on abrasive wear of grooved journal bearings, Wear. 376–377 (2017) 54–62. https://doi.org/10.1016/j.wear.2017.02.034.
[23] J. Sep, L. Galda, R. Oliwa, K. Dudek, Surface layer analysis of helical grooved journal bearings after abrasive tests, Wear. 448–449 (2020) 203233. https://doi.org/10.1016/j.wear.2020.203233.

[24] B. Vengudusamy, M. Von Hoersten, M. Schweigkofler, M. Kuhn, W. Litwin, Hydro lubricants: water-based lubricants for hydropower applications, in: Proc. HYDRO 2018, 15-17 October, Gdańsk, Pol., Gdańsk, 2018: pp. 1–7.

[25] W. Litwin, A. Olszewski, Assessment of possible application of water-lubricated sintered brass slide bearing for marine propeller shaft. 2012 | POLISH MARITIME RESEARCH 19 (4) , pp.54-61 https://doi.org/10.2478/v10012-012-0040-4

[26] W. Litwin, Water lubricated marine stern tube bearings - attempt at estimating hydrodynamic capacity, ASME/STLE International Joint Tribology Conference. 2010. Proceedings of the ASME/STLE International Joint Tribology Conference - 2009

[27] M. Damrat, A. Zaborska, M. Zajaczkowski, Sedimentation from suspension and sediment accumulation rate in the River Vistula prodelta, Gulf of Gdańsk (Baltic Sea), Oceanologia. 55 (2013) 937–950. https://doi.org/10.5697/oc.55-4.937.

[28] T. Leipe, F.X. Gingele, The kaolinite/chlorite clay mineral ratio in surface sediments of the southern Baltic Sea as an indicator for long distance transport of fine-grained material, Baltica. 16 (2003) 31–37.

[29] C.L. Dong, C.Q. Yuan, X.Q. Bai, Y. Yang, X.P. Yan, Study on wear behaviours for NBR/stainless steel under sand water-lubricated conditions, Wear. 332–333 (2015) 1012–1020. https://doi.org/10.1016/j.wear.2015.01.009.

[30] R. Orndorff, Water lubricated rubber bearings, history and new developments, Nav Eng J. (1985) 39–52.

[31] A. Barszczewska, Experimental Research on Insufficient Water Lubrication of Marine Stern Tube Journal Bearing with Elastic Polymer Bush, Polish Marit. Res. 27 (2020) 91–102. https://doi.org/10.2478/pomr-2020-0069.

[32] DNVGL-CP-0081. Synthetic bearing bushing materials, 2016.

[33] C. Yuan, Z. Guo, W. Tao, C. Dong, X. Bai, Effects of different grain sized sands on wear behaviours of NBR/casting copper alloys, Wear. 384–385 (2017) 185–191. https://doi.org/10.1016/j.wear.2017.02.019.

[34] C. Yang, X. Zhou, J. Huang, F. Kuang, X. Liu, Effects of sediment size and type on the tribological properties of NBR in water, Wear. 477 (2021) 203800. https://doi.org/10.1016/j.wear.2021.203800.

[35] R. Gheisari, A.A. Polycarpou, Three-body abrasive wear of hard coatings: Effects of hardness and roughness, Thin Solid Films. 666 (2018) 66–75. https://doi.org/10.1016/j.tsf.2018.07.052.

[36] R. Gheisari, A.A. Polycarpou, Tribological performance of graphite-filled polyimide and PTFE composites in oil-lubricated three-body abrasive conditions, Wear. 436–437 (2019) 203044. https://doi.org/10.1016/j.wear.2019.203044.

[37] M. Xue Shen, B. Li, S. Li, G. Yao Xiong, D. hui Ji, Z. nan Zhang, Effect of particle concentration on the tribological properties of NBR sealing pairs under contaminated water lubrication conditions, Wear. 456–457 (2020) 203381. https://doi.org/10.1016/j.wear.2020.203381.

[38] R. Prehn, F. Haupert, K. Friedrich, Sliding wear performance of polymer composites under abrasive and water lubricated conditions for pump applications, Wear. 259 (2005) 693–696. https://doi.org/10.1016/j.wear.2005.02.054.

[39] Z. Jia, Z. Guo, C. Yuan, Effect of Material Hardness on Water Lubrication Performance of Thermoplastic Polyurethane under Sediment Environment, J. Mater. Eng. Perform. 30 (2021) 7532–7541. https://doi.org/10.1007/s11665-021-05912-z.

[40] A. Barszczewska, E. Piatkowska, W. Litwin, Selected Problems of Experimental Testing Marine Stern Tube Bearings, Polish Marit. Res. 26 (2019) 142–154. https://doi.org/10.2478/pomr-2019-0034.

[41] E. Piątkowska, Influence of solid particle contamination on the wear process in water lubricated marine strut bearings with NBR and PTFE bushes, Polish Marit. Res. 112 (2022) 167–178. https://doi.org/10.2478/pomr-2021-0059.

The influence of polymer bearing material and lubricating grooves layout on wear of journal bearings lubricated with contaminated water

Wojciech Litwin, Michał Wasilczuk[1], Michał Wodtke, Artur Olszewski

Gdansk University of Technology
Faculty of Mechanical Engineering and Ship Technology
ul. Narutowicza 11/12
80-233 Gdańsk, Poland

Abstract

The goal of the present paper is to investigate wear properties of journal sliding bearing operating in the conditions of contaminated water lubrication. Several bearing materials and bearing sleeve designs (differing in the axial grooves position and their shape) were tested experimentally under typical operating conditions in a dedicated test rig, which was equipped with a lubricating system, enabling lubrication with contaminated water. Results of the tests show that water contamination has a strong impact on the wear of the bearing system elements. It was revealed that some of the tested materials are beneficial in such demanding conditions and demonstrate lower wear rates. The design of the bearing bush also seems to have an impact on the wear, because bearings of different designs made from the same material demonstrated differences exceeding 100%. Higher water velocity in the lubricating grooves helps to minimize the wear of the stainless steel shaft. This was also confirmed by numerical simulations.

Keywords

polymer sliding bearings, water lubrication, hard particles, experimental testing

1 Introduction

The conditions for the generation of full film lubrication in sliding bearings are commonly known and result directly from solution of the Reynolds equation. However, in practice the operation of hydrodynamic bearings depends on many design and operational factors. One of them is the lubricant condition. It is common to assume that the lubricating fluid is free from contamination. However, this assumption is usually not true, even for new lubricating oils, the presence of a certain number of contaminant particles is allowed, depending on the specific requirements for particular applications [1]. The increased amount of contaminants in the lubricant may result from wear of the friction

[1] corresponding author, email: michal.wasilczuk@pg.edu.pl

surfaces, failure, and ineffectiveness of the seal or natural conditions, such as in the case of marine bearings or hydropower turbine bearings lubricated with unfiltered water from the environment. Hard particles getting into the lubrication gap of the hydrodynamic bearing damage or wear its sliding surfaces. The unfavorable influence of contaminants in the oil is usually limited by the use of bearing alloys, such as Babbitt alloys, one of the tasks of which is to allow the embodiment of solid particles [2]. Oil lubricated bearings are also used in shipbuilding, mainly because of their high durability and the absence of shaft corrosion [3]. However, this is a costly and complex solution due to the need to use reliable seals against oil leakages, while even small oil leakages of oil can be dangerous to the environment.

The influence of an increased amount of contaminants in the lubricating fluid on the operation of hydrodynamic bearings has been the subject of research for many years. Early experimental work concerned mainly oil-lubricated journal bearings [4–11] and was supplemented by theoretical studies of selected aspects of the influence of pollutants on the operation of hydrodynamic bearings [12–17]. For the purpose of experimental studies, various types of pollutants were introduced into the lubrication system (diatomaceous earth, steel machining chips, weld spatter, flyash, Al_2O_3, Air Cleaner Fine Test Dust, iron or quartz - SiO_2 particles, ISO Medium Test Dust) with a weight concentration of 0.0012% [10] up to 1.0% [4]. In other researches larger size contaminants were added, i.e., steel machining chips (a few to a dozen or so particles) or weld spatter [5]). The particles varied in size - from 1 µm [4] to even 1.4 mm [5]). The test results confirmed the negative impact of the presence of impurities in the oil on the bearing's performance, including an increase in resistance to motion (depending on the concentration of particles in oil [10, 12]), an increase in operating temperature [11] and increased surface wear. It has been proved that the wear mechanism depends on the particle size (mainly the possibility of their getting into the lubricating film [5, 11]) and their hardness. For example, the results from Vikström, et al. [9] indicate that hard Al_2O_3 particles can cause intensive abrasive wear to the bearing surface, while impurities with lower hardness (i.e., iron particles) result in much less wear in the form of polishing without the risk of failure. The wear of sliding surfaces also depends on their hardness and the hardness of dirt particles in the oil [6–8]. According to the work by Xuan et al. [8], the shaft wear is the lowest when it is much harder than the bearing surface or when its hardness is close to or greater than that of the particles. Khonsari et al. [13–15] investigated the influence of contamination on the occurrence of the phenomenon of scuffing, a wear process that involves a local increase in surface temperature above the critical temperature (flash temperature) at which the oil loses its protective properties, which causes the loss of the boundary layer and surface failure. Bou-Said et al. [16, 17] determined theoretically the operating parameters of a bearing lubricated with the lubricant in which rheological properties are changed due to the presence of impurities, assuming significant contents of particles in the oil (10-30 wt.%). The experimental results of the influence of

contaminants in the oil on the performance of hydrodynamic bearings (summarized synthetically in [18]) became the basis for determining the requirements of oil filtration for the safe operation of hydrodynamic bearings [11, 19]. A separate demand raised in the research was a bearing structure that would minimize the negative effects of the presence of contaminants. Dadouche et al. [20] examined bearings with surface texture and Sep et al. [21–23] bearings with a special helical groove machined on the shaft. The results of these works indicated that it is possible to reduce the surface wear caused by particles in the oil compared to cylindrical bearings by changing the design of the bearing.

Recently, due to the growing importance of environmental protection, intensive research has been carried out on the feasibility of replacing lubricants that are potentially dangerous to the environment with other ecological liquids. More environmentally friendly lubricants based on water, esters, glycols, etc. (so-called EAL - environmentally acceptable lubricants) are used. It is possible to replace mineral oil with an environmentally friendly lubricant without the need to modernize bearings with whitemetal bushings [24]. Water-lubricated bearings are also developed, operating in a closed circuit system, where filtered fresh water is circulating in the sealed system, or in an open system, when the surrounding water serves as a bearing lubricant [25, 26].

In the case of bearings operating in open systems (e.g., stern tube bearings of propeller shafts, guide bearings of water turbines), the presence of contaminants that occur naturally in water is inevitable [27–29]. General conclusions about the influence of contamination on the performance of oil-lubricated hydrodynamic bearings can, according to the authors, be correlated to water-lubricated bearings only to a limited extent. Both lubricants differ significantly in physical parameters and lubricity and the materials from which the bearings are made are different. In the case of water-lubricated bearings, NBR rubber is often used, one of the advantages of which is greater tolerance to lubrication with contaminated liquid, as compared to lignum vitae [30]. Other materials, such as polymers or sintered brass [26,31] are also used. It is worth noting that the existing practical recommendations for water-lubricated bearing materials do not consider the problem of operation with contaminated lubricant [32].

The literature provides extensive results of tribological tests of materials used for water bearings carried out under contaminated lubrication conditions. Most often, sediments obtained from the natural environment were used for the research, e.g., Yangtze River [29, 33, 34] or the Gulf of Mexico Coast [35, 36], but also, for example, Al_2O_3 [37] or quartz particles [34]. The average particle size distribution of the impurities was usually in the range from a few to a maximum of 300 µm. Tribological tests of NBR rubber in the conditions of lubrication with contaminated water with a concentration of 1.1 wt. % were carried out [29, 34]. The results indicated a strong dependence of the wear and friction coefficient on the concentration and size of the particles. Solid particles in water destroyed the

lubricating film causing abrasive wear. At the same time, no traces of transfer of the rubber material to the mating surfaces (stainless steel, brass) were found. Yang et al. [34] performed a comparative study of the impact of the type of impurity on NBR wear. The obtained results indicated that material wear as a result of SiO_2 particles of a given size was greater than that in the case when the natural sediments of the same grain size also contained clay in addition to SiO_2. In the case of polymeric materials, tribological tests under the conditions of water lubrication with contaminants were aimed, among others, at investigating the effect of filler contents and polymer hardness on their wear rate [38, 39].

All the tribological tests of NBR and polymers described above were carried out on tribometers and not on the bush-shaft arrangement as in the journal bearing. For this reason, the test conditions reproduced the bearing operating conditions only to a limited extent, because the configuration of the contact was different, and thus the transport of pollutants in the film. In order to fully take into account the operating conditions of the bearing, it is necessary to conduct experimental tests on real objects, which requires special test stands [40] and the results of such works available in the literature are sparse [41].

The main goal of the present research was to investigate the effect of the material and the polymer sleeve design on the intensity of wear of journal bearing systems lubricated with contaminated water. Due to the complexity of the phenomena taking place in operation with contaminated lubricant it was decided to test bearing models similar to the real polymer bearings. Three materials and four designs of the bearing (differing mainly with the number, shape, and arrangement of axial lubricating grooves) were tested experimentally under typical operating conditions of water lubricated bearings (in terms of the sliding speed and specific load) in order to find the influence of polymer bearing material and bearing design on the intensity of wear of both, polymer bearing bush and the steel shaft. Experimental investigations, containing a series of long duration tests, were carried out on the specialized test stand equipped with a separate lubricating system, enabling lubrication with the contaminated water.

Experimental investigations were supplemented with CFD (*Computational Fluid Dynamics*) calculations of the water flow in selected bearing designs. The goal of the theoretical research was to investigate the effect of the bearing geometry on the water streamlines and thus on the potential trajectory of the solid particles dispersed in the lubricant (which is mainly driven by water flow).

2 Materials and Methods

2.1 Test stand

Experimental tests were carried out on the hydrodynamic journal bearing test stand allowing for long-term tests under lubrication with contaminated water (Fig. 1). In order to provide a homogeneous

distribution of the contaminating sand particles (mainly SiO_2), two tanks with mixers were used together with a peristaltic pump supplying contaminated water directly to the test bearing housing, which is shown in a schematic view (Fig. 1 b). Lubricating water was then passing axially through the grooves in the bearing bush and to the lubricant tank, in a similar manner as in a real ship or water turbine (see the cross-section of the test head - Fig. 1 c). An excess of the lubricating water was returning to the system via an outflow. Test bearing was loaded by a hydraulic piston pressing the shaft via a roller element bearing (shown in Fig. 1 b). The housing design provided the ability to tilt, which prevented edge loading of the bearing bushes. Test shafts were designed as exchangeable stainless steel sleeves to test a new set of a bearing sleeve and a shaft each time.

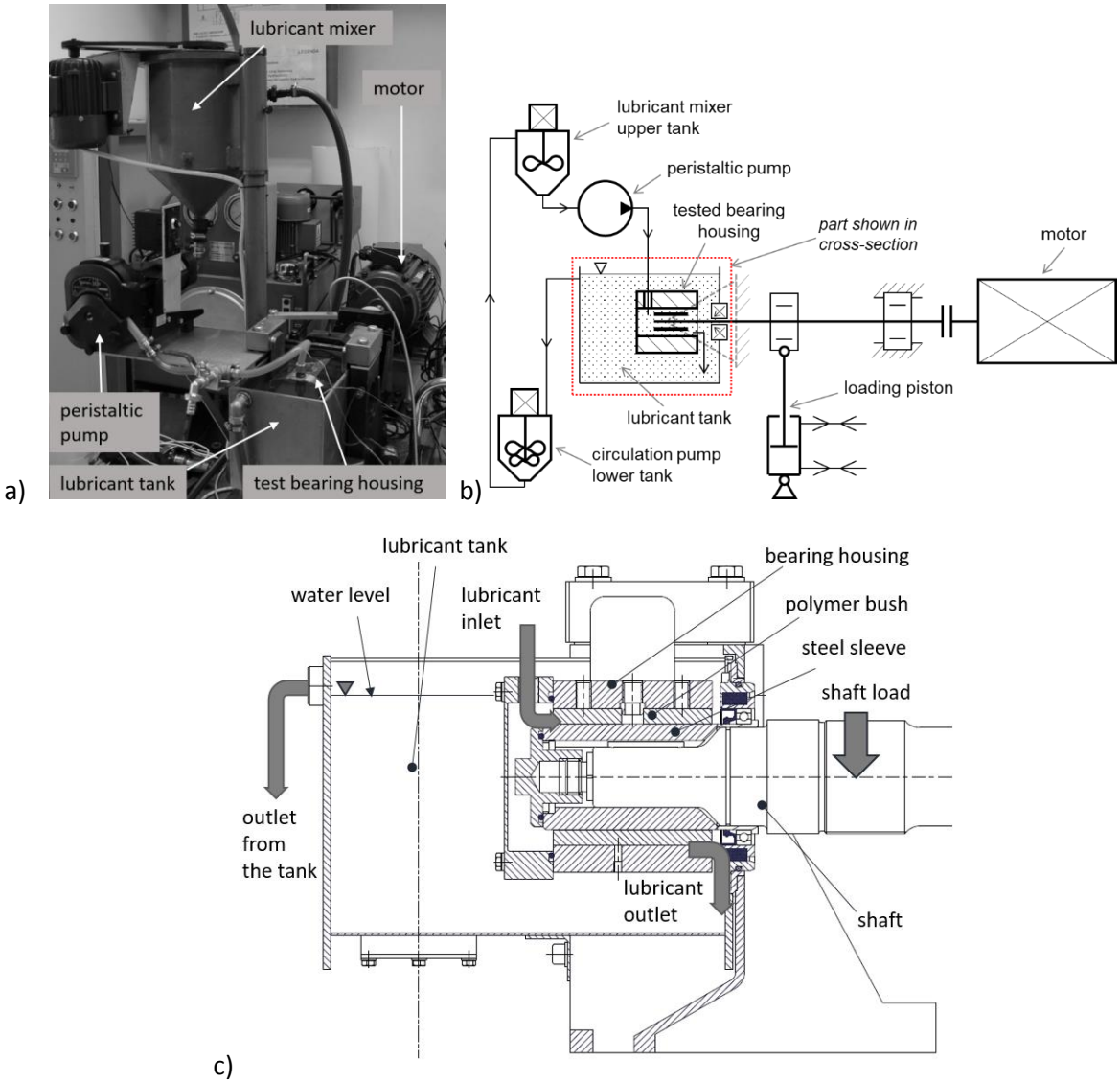

Fig. 1. Test stand; a) general view, b) schematic view, c) test head cross-section.

2.2 Tested bearings

Four designs of bearing sleeves (originated from real bearing applications) were tested. Test sleeves differ in the shape and number of open axial grooves (as shown in Fig. 2):

- Bearing with two cylindrical grooves,
- Bearing with six rectangular grooves in the upper half of the bearing and chamfered groove edges (1x45°),
- Bearing with six rectangular grooves in the upper half of the bearing and sharp groove edges,
- Bearing with six rectangular grooves with wider spacing of grooves, including two at the lower half of the bearing.

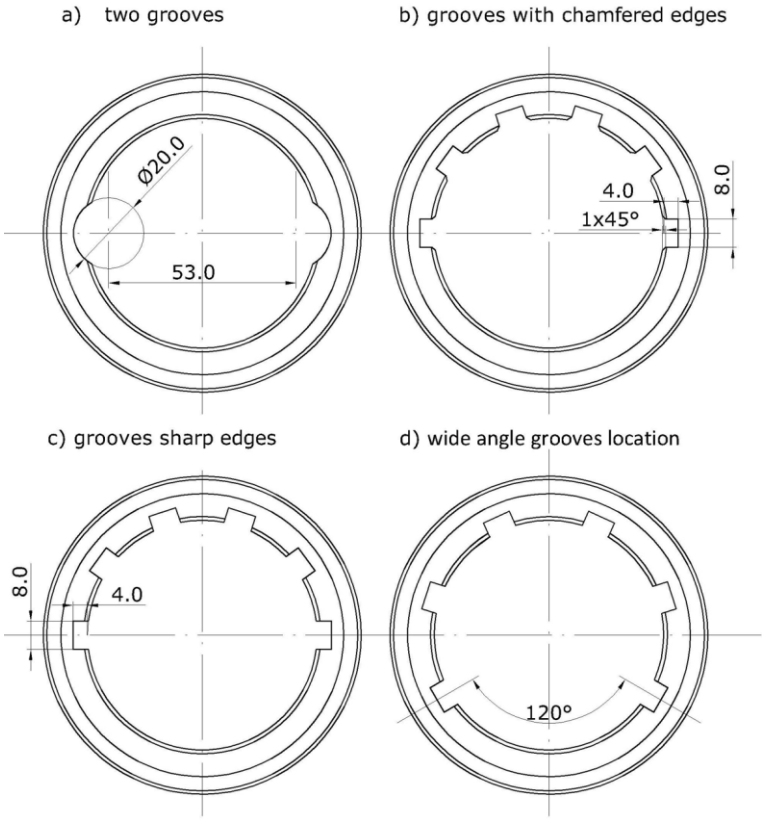

a)

Fig. 2. Test bearings a) two grooves, b) upper half grooves with chamfered edges, c) upper half grooves with sharp edges, d) wider spacing of the grooves.

There are no clear recommendations concerning certain applications of the presented bearing geometries and various manufacturers, according to their own experience, use different layout of the lubricating grooves, as well as the chamfered or sharp edge of the groove, as shown respectively in Fig 3 a and b.

It is not known how the chamfers vs. sharp edges of the groove influence the wear of the bearing system lubricated with a contaminated fluid. It seems, that in the case of chamfered grooves solid particles can enter the film more easily, due to the converged wedge in the entry zone, while sharp

edges will prevent the solid particles from entering the film, but these speculations are not supported by any research results, theoretical or experimental known to the authors.

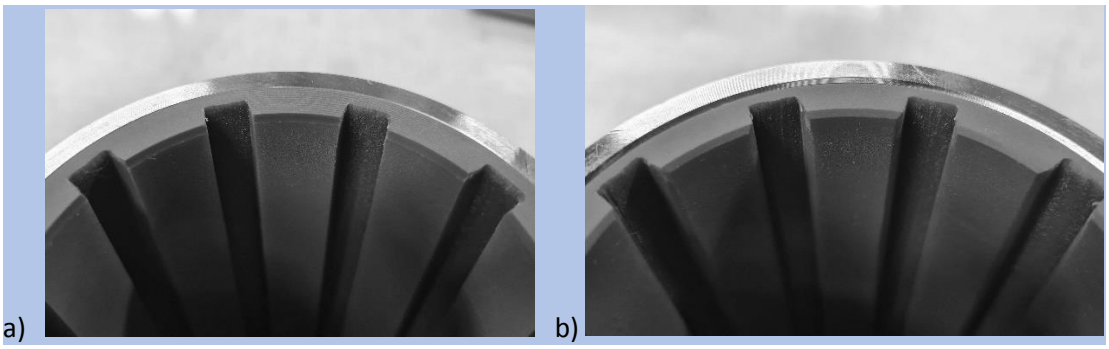

Fig. 3. Two styles of the lubricating groove edges a) sharp edges, b) chamfered edges.

The bush with each groove design (four different geometries, as shown in Fig. 2) was made from three different types of commercially available bearing materials:

- polymer material (marked as A),
- three layer composite material with rubber layer lined with filled PTFE (marked as B),
- composite material based on a special synthetic fabric impregnated with a thermo-setting resin (marked as C).

The main characteristics of the bearing sleeve materials are collected in Table 1, hardness of the polymer materials is not given in manufacturers' data. The exchangeable journals were made of austenitic stainless steel X10CrNi18-8, equivalent to AISI 301 with the hardness of 25-26 HRC, machined to approximately Ra0.5 roughness. Chemical composition of steel sleeve is given in Table 2,

Table 1. Bearings material data.

Material type	Modulus of elasticity [MPa]	Water swell [%]	Thermal expansion coefficient x 10-5 [1/K]
thermoplastic polymer (A)	610	1.6	20
3 layers composite(B) (PTFE/NBR/bronze)	770 / 40 / 103 000	0 / 0 / 0	12.4 / 17 / 2.2
thermoset polymer with fibers (C)	2800	0.5	5 - 10 (depending on direction)

Table 2. Chemical composition (wt%) of stainless steel journal.

C	Si	Mn	Ni	P	S	Cr	Mo	N
0.05 - 0.15	max 2	max 2	6 - 9.5	max 0.045	max 0.015	16 - 19	max 0.8	max 0.11

2.3 Experimental procedure

Additionally to a problem of lack of standards for testing bearings lubricated with contaminated fluid, there is also an ambiguity of type and quantity of hard particles dispersed in a lubricating water for tests. The authors collected samples of water from a small river after a heavy rainfall. Analysis of the amount of contaminating solid particles showed that their concentration could be as large as 5 cm³ / liter.On one hand this was the amount practically occurring in natural conditions, on the other hand this amount caused quite fast wear of the polymer bushes, as the pilot tests showed. Tests conditions and details of lubricating water finally used in the research are collected in Table 3.

Table 3. Bearings tests conditions and details of applied lubricating medium (contaminated water).

Load (specific load)	Speed	Water flow	Particles concentration	Volume of solid particles	Water volume in the system
4480 N (0.65 MPa)	430 rpm	3 l/min	0.5 ‰	5 cm^3/liter	10 liters

The contaminant is mainly composed of SiO_2 particles. Examples of the particle size distribution and the microscopic photo of the particles is shown in Fig. 4. Microscopic images show that the grains are rounded, without sharp edges, which is typical of sedimentary material carried by rivers.

Water with solid particles was in constant motion in the system, due to stirring in a lubricant mixer, to prevent sedimentation of particles. The total time of one wear test was 70 hours of operation including the running-in phase (Table 4). Sliding distance under lubrication with contaminated water was equivalent to approximately 315 000 m. During each test, the lubricating water was changed four times (every 15 hours of operation) in order to introduce a new quantity of solid particles, which during the operation were constantly degraded as a result of wear.

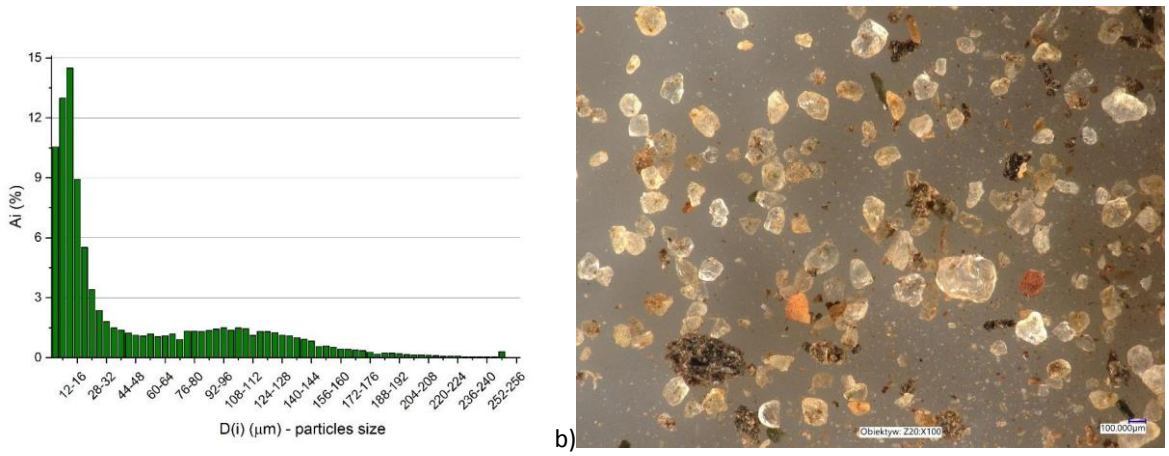

a) b)

Fig. 4. Solid particles added as water contamination; a) example of particles size distribution in one portion of contamination, b) microscopic view (x100).

Table 4. Testing procedure.

#	Description	Duration	Comment
1	Running-in stage	10 h	two phases (each 5h long); speed 260 and 430 rpm; load 4480 N (0.65 MPa) water without particles
2	Wear test stage	60 h	four phases (each 15h long); speed 430 rpm; load 4480 N (0.65 MPa) fresh lubricating medium with solid particles in each phase

Linear wear of the bearing sleeves was evaluated by wall thickness measurements before and after the test, in three cross sections – one vertical, in line with the load, and two other in the cross sections 15° apart (Fig. 5).

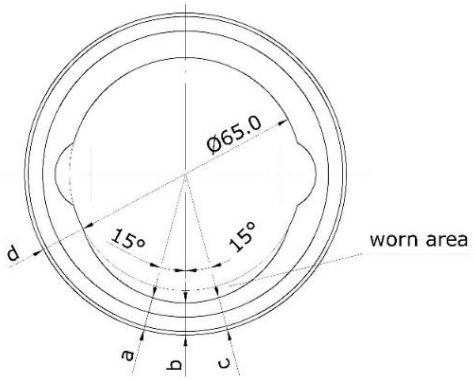

Fig. 5. Schematic of the bearing sleeve wear measurements.

Measurements were done in front and in the back of the bearing sleeve before and after the wear test. Wear in each location was evaluated as the difference between the thickness of the bush before and after the tests. Representative linear wear of the bearing sleeve shown in the paper was calculated as an average of wear in six positions, where appropriate the graphs with the results show the standard deviation of the evaluated wear. The condition of the steel shaft was also checked - the surface profile of the shaft was measured in the axial direction, with the use of a profilometer which allowed us to evaluate its linear wear (with the use of Jenoptik Hommel Etamic T8000 contact profilometer). In this way the wear of both polymer bearing sleeves and steel shafts were evaluated, as well as the changes in the roughness of the steel shafts. Finally, the program of the experimental tests covered five bearings sleeves made of each material: four designs (as shown in Fig. 2) lubricated with contaminated water, and the sleeve with two grooves (Fig. 2a) was additionally tested under water lubrication without contaminants. This allowed assessing the influence of the presence of solid particles in the lubricating water on bearing wear.

3 Results and discussion

3.1 Effect of contamination

A comparison of the measured linear wear of the bearing sleeve and steel shaft for clean and contaminated water lubrication is shown in Fig. 6. It was tested with the use of the bearing bushes with two cylindrical grooves (style a) made from each of three materials. The results revealed that, as far as sleeve wear is concerned, there is a predominant influence of the material. Material A demonstrates wear (maximum measured wear ~165 µm), which is an order of magnitude larger than that of material B and more than two times larger than that of material C. The influence of the cleanliness of the lubricant is significant but smaller than the effect of the material. The assessed linear wear of the shafts was significantly smaller in comparison to bearing sleeves wear (maximum measured value ~5 µm). On the other hand, wear of the steel shafts seems to be much less affected by the bush material type, than by the water contamination.

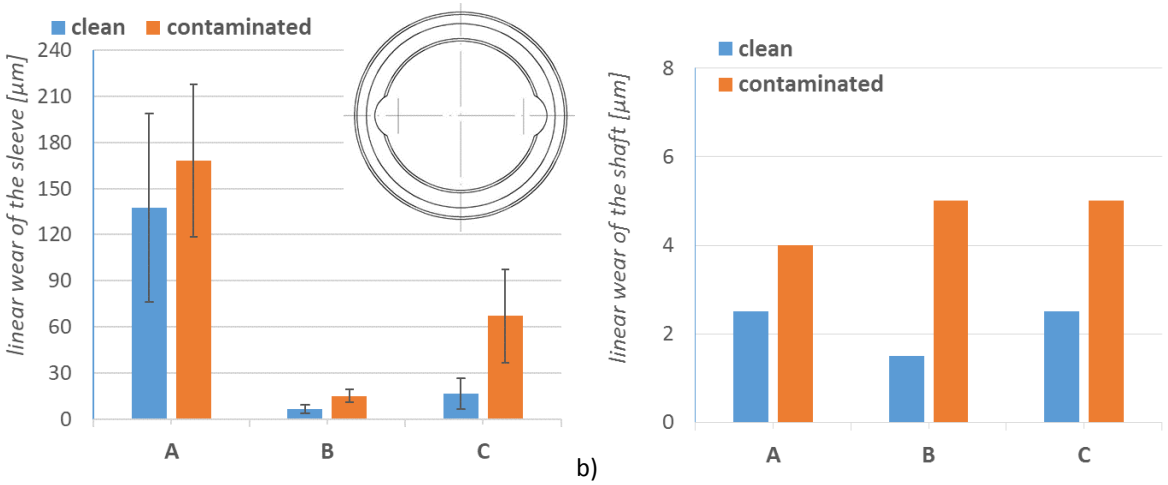

Fig. 6. Comparison of the linear wear a) of the bearing sleeve – with standard deviation bars, and b) the steel shaft, lubricated with clean and contaminated water for different materials (A, B, C) and two cylindrical grooves geometry (style a).

In Fig. 7 photographs of the sleeves after tests are shown for all tested materials. One can see different patterns of wear between the various materials, with quite heavy wear of material A. Wear of bushes in clean and contaminated water does not differ significantly but the angular extent is slightly larger for contaminated water lubrication. In all cases, worn areas are smoother than the bush surface outside the wear area. This was also confirmed by the roughness measurements after the tests.

a)

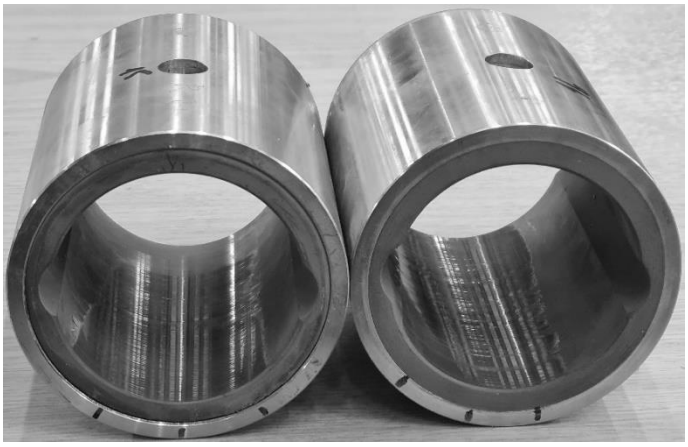

b)

c)

Fig. 7. Photographs of the bearing sleeves after tests lubricated with clean water (left-hand side) and with contaminated water (right-hand side): a) made of polymer (material A), b) 3 layers type (material B), c) made of thermoset composite (material C).

The wear process has also a significant effect on components' surface roughness parameters, which is shown in Fig. 8. For both lubricant conditions, clean and contaminated, the polymer bush roughness parameter is significantly decreased during the test. The result differs much for the steel shaft roughness (Fig. 8 b), its roughness remains almost unchanged when it is lubricated with clean water (except for the shaft rubbing against material C), while the roughness increases when the shaft is

lubricated with the contaminated water, by 20% (for material C) to approximately 50% (for materials A and B).

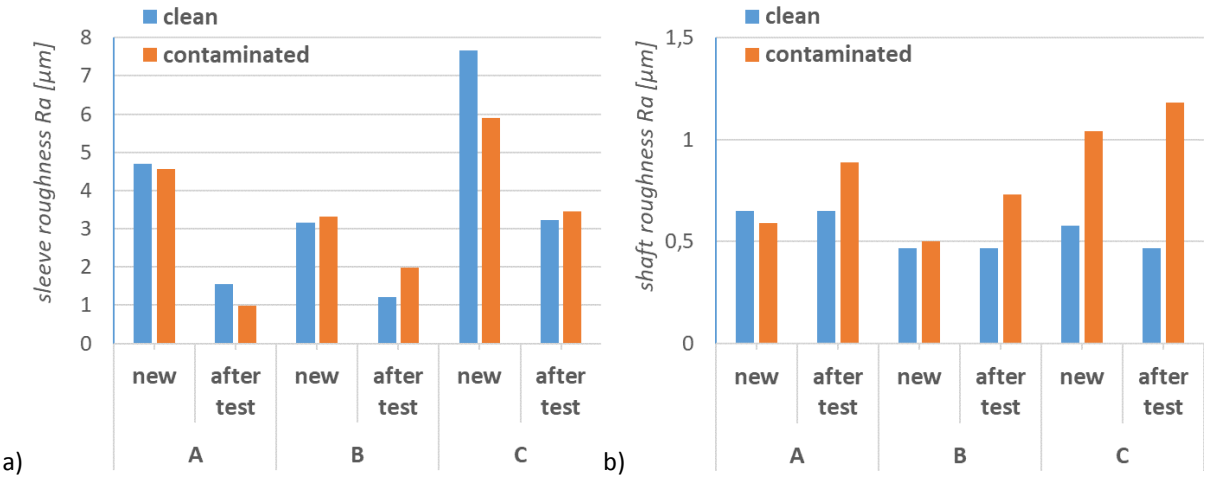

Fig. 8. Roughness Ra parameter measured before and after the tests in clean and contaminated water; a) bushes, b) shafts.

Images of the worn shaft are presented in Fig. 9, after the test in clean and contaminated water lubrication, one can observe more circumferential scratches after lubrication with contaminated water.

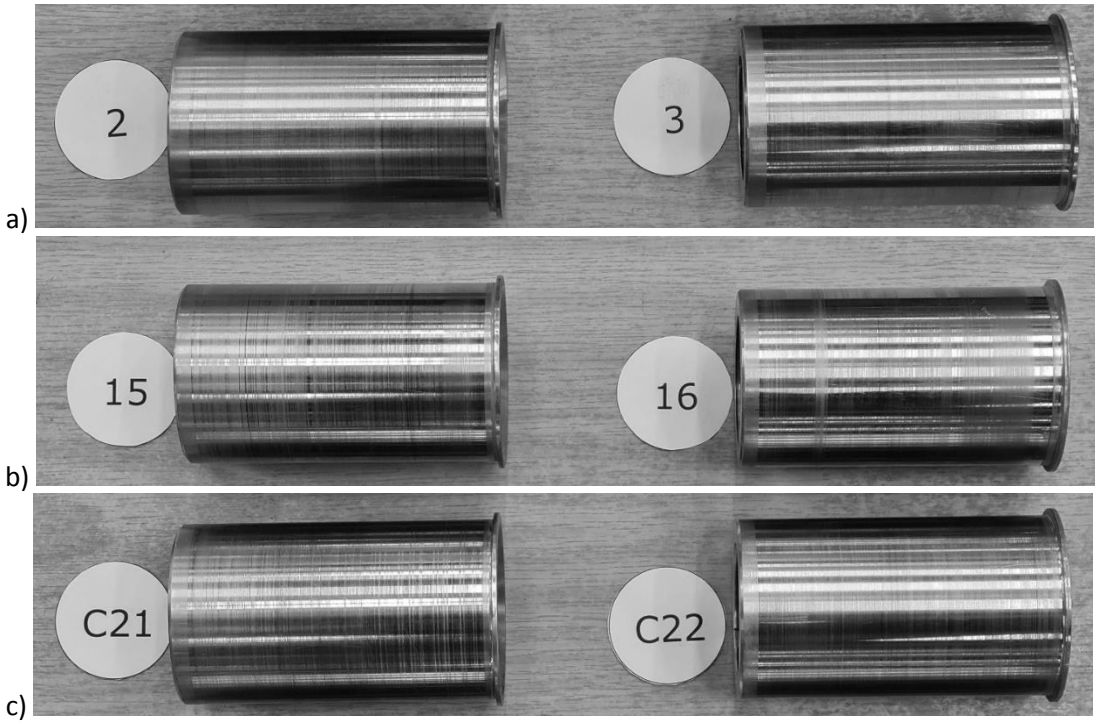

Fig. 9. Pictures of the shaft after tests with clean (left-hand side) and contaminated water lubrication (right-hand side); a) tested with sleeve A, b) tested with sleeve B, c) tested with sleeve C.

3.2 Effect of bearing sleeve geometry

Fig. 10 a) shows the linear wear of the polymer bearing sleeves made of the tested materials (A, B, and C) in various geometrical configurations (a, b, c, d). It can be noticed that the influence of the type of material is more pronounced than the influence of the sleeve geometry. Polymer material A has a linear wear almost an order of magnitude greater than the other tested materials, with the multi-layer material B has a slightly smaller wear than the composite material C. The influence of the configuration of the lubricating grooves is also visible, especially for polymer material A, but it is not so significant. The configuration with two cylindrical cross-section grooves seems to be only slightly more favorable than the others, this is noticeable for the two materials (A and B), whereas in the composite material C the influence of the configuration of the grooves is not very pronounced, with the wear in all configurations very close to one another. Macroscopic image of the worn areas confirms this finding, because the worn areas for each material look similarly in terms of smoothness and number of visible deep scratches, which can be observed on the surface. The wear is uniform along the bush axis.

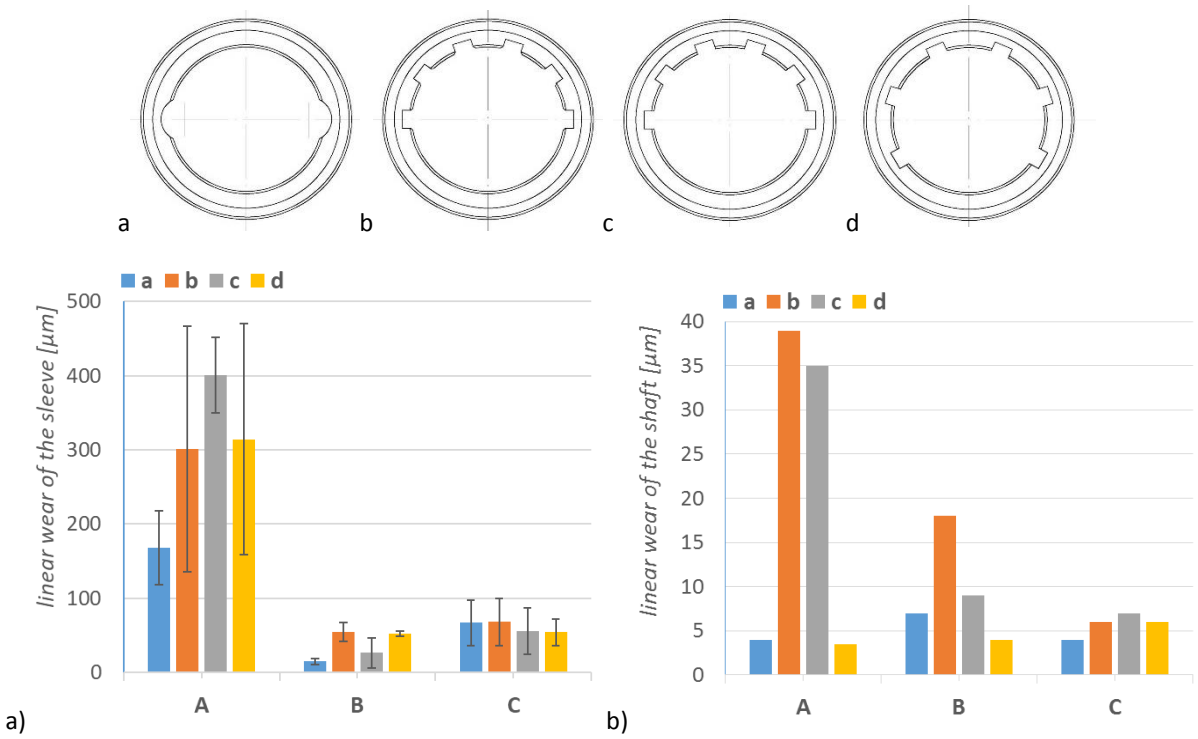

Fig. 10. Comparison of the linear wear: a) of the bearing sleeve – with standard deviation bars, and b) the steel shaft, both lubricated with contaminated water for different materials (A, B, C) and geometries of the sleeve (styles a, b, c, d).

Wear of the steel shaft is shown in Fig. 10 b), it is an order of magnitude smaller than that of the polymer bush, but in technical circumstances its wear is very important, because the shaft is usually much more difficult and costly to replace than the polymer bush. Looking at the worn surface of the shafts one can observe quite regular wear marks with some deeper scratches distributed randomly along the contact area. The linear wear of the steel shaft to some extent also depends on bush material, but the differences between shafts rubbing against the various materials are much smaller.

A larger influence of the lubricating grooves configuration can be observed, with cylindrical grooves (a) and the grooves with wider spacing (d) being the configurations yielding smaller wear in all three material cases, than these with sharp or chamfered edges of the grooves located only in the unloaded half of the bush (b and c). The style of the edge (sharp vs chamfer) does not seem to be a significant factor in all materials – sharp edges are considerably better for materials A and B, while in material C, an opposite, but much smaller difference is observed.

3.3 CFD analysis of lubricant flow in the bearing

In order to investigate the structure of the fluid flow in the bearing, and thus the potential influence of the internal geometry (shape and number of grooves) on the movement of contaminants carried with the lubricating water, numerical analyzes were performed using CFD (Computational Fluid Dynamics). It was assumed that the lubricating water flow was incompressible, turbulent (SST model) taking into account cavitation (Rayleigh-Plesset model). The calculations were made for two cases of bearing geometry: cylindrical grooves (style a) and six rectangular grooves with sharp edges (style c). Water flow was modeled in the gap, axial grooves, and in the inlet and outlet areas of the bearing gap (Fig. 11), with the following assumptions:

- viscosity of 0.001 [Pa s] at 20^{o}C,
- inlet with a flow rate of Q = 3 l / min,
- outlet with forced axial flow in the direction of the z-axis,
- the surface of the shaft rotated around the bearing axis with the angular velocity ω, with the condition of no slippage,
- all external walls of the model were assumed to be stationary with the condition of no slippage on the wall.

To obtain the appropriate quality of the elements, the computational mesh, depending on the analyzed case of bearing geometry, was divided into 2.3 to 2.6 million of finite volumes (12 divisions across the thickness of the film). Additional volumes at the inlet and outlet of the slot (25 mm axial length, 80 mm OD) allowed to move the boundary conditions (Inlet, Outlet) away from both ends of the lubrication gap and to calculate the desired water flow conditions at the edges of the slot and axial grooves. The dimensions of the bearing in the CFD calculations (diameter, length) and axial grooves were assumed the same as in the laboratory tests (see Fig. 2), the diametral clearance was 0.15 mm.
The use of CFD allows for the analysis of the bearing operation in the conditions of fluid film friction. For this reason, the calculations were carried out assuming that the minimum film thickness was 10 μm and selecting the bearing attitude angle in the course of iterative calculations so that the resultant

hydrodynamic force had a vertical direction (horizontal component <± 1 N), the shaft rotational speed in the calculations was 1000 rpm.

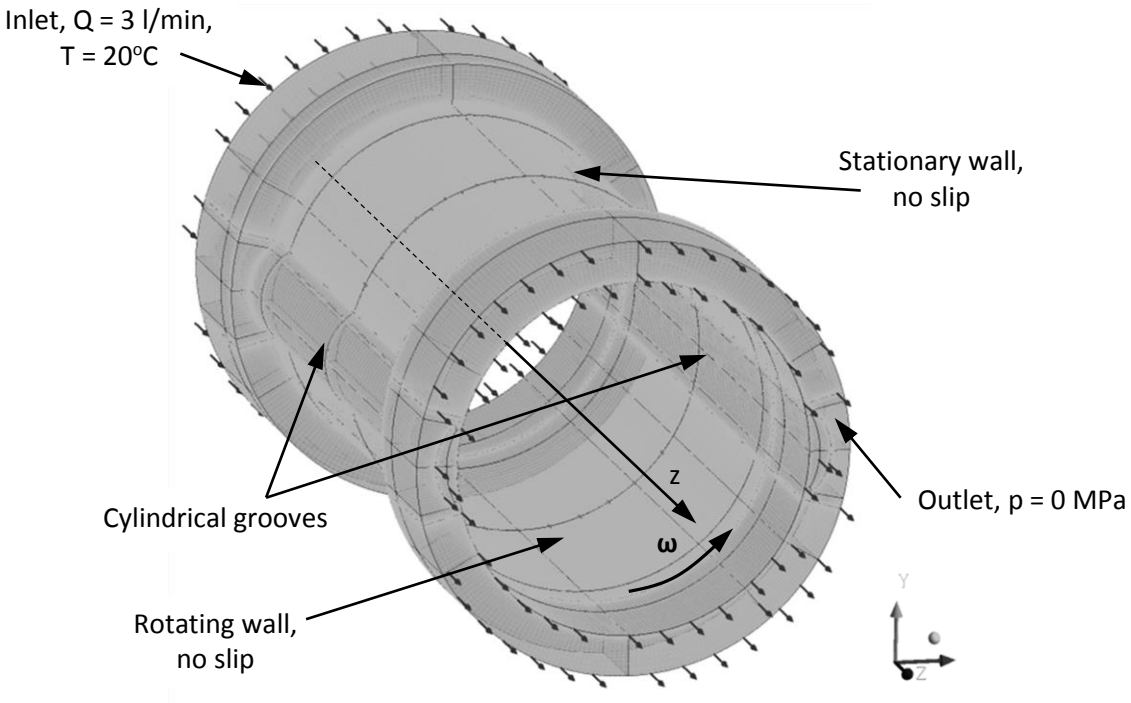

Fig. 11. Computational mesh for CFD calculations with marked boundary conditions – geometry with the cylindrical grooves.

Bearing load with these assumptions was much lower than the one applied in the experiments, nevertheless, the conclusions drawn from the results (flow pattern) are still valid, since, as confirmed with CFD calculations, water flow took place almost only through grooves.

Results of CFD calculations of the velocity streamlines and axial velocity profiles in groves on the selected axial cross sections of the bearing are shown respectively in Fig. 2 and Fig. .

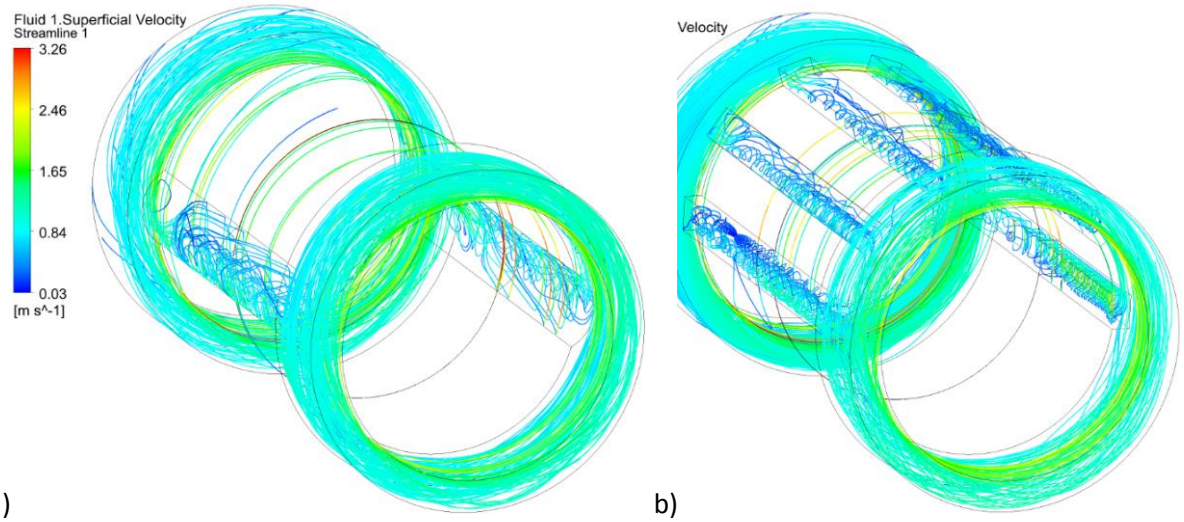

a) b)

Fig. 12. Streamlines of the lubricant, view from the outlet side a) cylindrical grooves, b) six rectangular grooves with sharp edges.

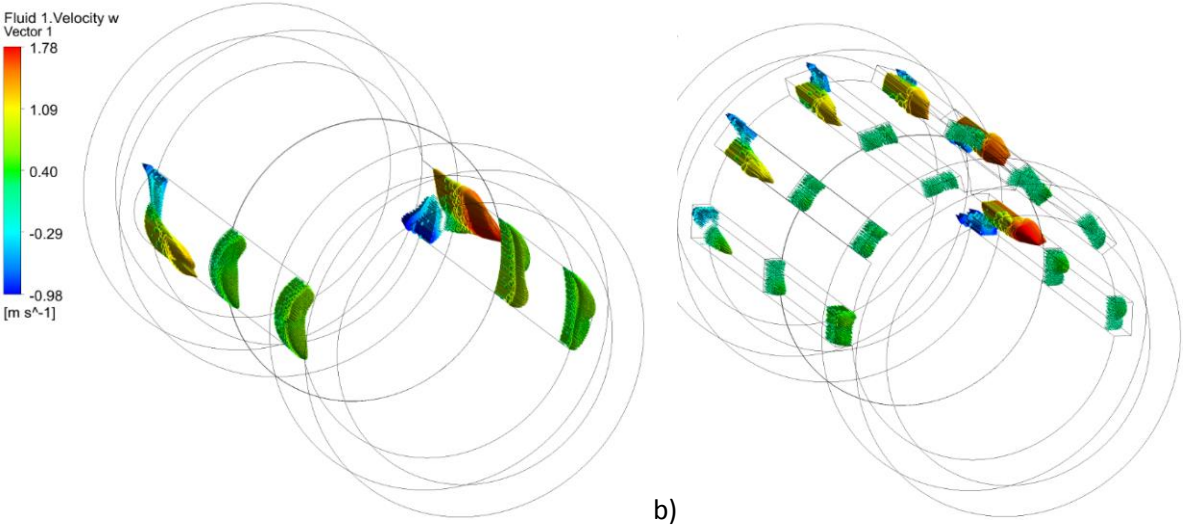

a) b)

Fig. 13. Axial velocity of the fluid in the grooves at three cross sections (inlet, mid-plane, outlet), view from the outlet side; a) cylindrical grooves, b) six rectangular grooves with sharp edges.

The calculated flow lines for the flow of water in the bearing reveal, in addition to the axial flow between the inlet and the outlet, a strong eddy flow inside the grooves due to the rotational movement of the shaft. Overall, it can be stated that the flow structure in the grooves is very complex. A similar picture was obtained both for the geometry of the bushings with cylindrical and rectangular grooves.

Analysis of the results of the axial velocity distribution in the grooves reveals that there are backflows in the inlet area and the flow becomes unidirectional over the entire cross-section of the grooves in the center and outlet areas of the bearing. The quantitative analysis of the obtained flow results is summarized in Table 5.

In the table, detailed values of the calculated flow rates and average axial velocities at the bearing mid-length cross-section were presented separately for each groove and water film section (TOP – thickest film zone and BOTTOM – thinnest film zone). The speed of the water in the grooves was used to analyze the potential of the flow to transport the contaminating particles.

Regardless of the analyzed geometry of the bearing, the axial flow of water takes place almost entirely through the grooves. Higher flow rates Q (and the closely related mean axial flow velocities Vz) were observed for the geometry with cylindrical grooves as compared to the geometry with rectangular grooves. This is caused by the fact that the cross-sectional area of the grooves is approximately two times smaller in cylindrical grooves, which results (for the same forced flow rate) in higher axial flow velocities. This is, most likely, the main circumstance that prevents contaminants carried by the lubricating water from getting into the fluid film. The higher flow velocity (kinetic energy) allows contaminants to be transported more efficiently between the bearing inlet and outlet.

Table 5. Results of CFD calculations of parameters of the bearings with different groove arrangements

			cylindrical grooves (geometry a)	rectangular groves with sharp edges (geometry c)
Angular position of minimum film thickness Kąt h_{min} - γ		deg	310.7	313.2
Vertical load F_Y / mean pressure		N / MPa	572.2 / 0.084	542.9 / 0.079
Cross section of a single groove		mm^2	49.5	32
Total cross-section of all grooves		mm^2	99	192
water flow Q / average axial velocity V_z (at mid bearing length cross section)	Film TOP	l/min / m/s	0.003 / ~ 0	0.007 / ~ 0.02
	Film BOTTOM		~ 0 / ~ 0	~ 0 / ~ 0
	Groove 0°		1.688 / 0.56	0.549 / 0.28
	Groove 36°		-	0.554 / 0.28
	Groove 72°		-	0.448 / 0.22
	Groove 108°		-	0.458 / 0.23
	Groove 144°		-	0.525 / 0.26
	Groove 180°		1.309 / 0.42	0.459 / 0.23
	Total		~ 3 / -	~ 3 / -

4 Conclusions

The obtained results can be summarized as follows:

- Lubrication with water contaminated with hard particles is a frequently encountered regime of operation of marine and hydropower ecological bearings, but little literature data is published.
- Quite expectedly wear rate in contaminated water was larger, and the wear rate of the polymer sleeve bush and steel shaft increased by 40-300% and 30-400% respectively in comparison to clean water lubrication.
- In the contaminated water, bearing material choice had the largest influence on the wear rate of the bearing bush – various tested bearing materials demonstrated the wear rate differing by a factor of 3 to 8.
- The influence of the bearing design (the arrangement of the lubricating grooves) was also considerable – the differences between the bearings made from the same materials and differing by the design were over 100% in some cases – this finding necessitates the collection of component level testing data for reliable determination of wear rates of composite bearing materials
- In the case of steel shaft, the influence of bearing bush polymer material was less significant than the influence of groove design.
- The expected influence of chamfer vs. sharp edge of the grooves on wear rate was not consistently confirmed; and
- CFD calculations also show that the advantage of cylindrical grooves may be due to higher water velocity in the lubricating grooves, helping to wash out the contaminating particles.

5 Acknowledgments

This work was a part of research grant no. 2016/23/B/ST8/03104 entitled “Research on water-lubricated sliding couples in unfavorable operating conditions” financed by the Polish National Science Centre.

Computations were carried out using the computers of Centre of Informatics Tricity Academic Supercomputer & Network (TASK)

6 References

[1] D. Margaroni, Oil cleanliness, Lube-Tech. 25 (2002) 1–4. https://www.lube-media.com/lube-tech/.

[2] W.M. Hannon, M.J. Braun, Hydrodynamic Journal Bearings, Encycl. Tribol. (2013) 1736–1748. https://doi.org/10.1007/978-0-387-92897-5_41.

[3] W. Litwin, Experimental research on marine oil-lubricated stern tube bearing, Proc. Inst. Mech. Eng. Part J J. Eng. Tribol. (2019). https://doi.org/10.1177/1350650119846004.

[4] S.A. McKee, Effect of abrasive in lubricant, SAE Trans. (1927) 73–77.

https://doi.org/10.4271/270009.
[5] R.C. Elwell, Foreign Object Damage in Journal Bearings., Lubr. Eng. 34 (1978) 187–192.
[6] A. Ronen, S. Malkin, Wear mechanisms of statically loaded hydrodynamic bearings by contaminant abrasive particles, Wear. 68 (1981) 371–389. https://doi.org/10.1016/0043-1648(81)90183-6.
[7] A. Ronen, S. Malkin, Investigation of Friction and Wear of Dynamically Loaded Hydrodynamic Bearings With Abrasive Contaminants, J. Tribol. 4 (1983) 559–567.
[8] J.L. Xuan, I.T. Hong, E.C. Fitch, Hardness effect on three-body abrasive wear under fluid film lubrication, J. Tribol. 111 (1989) 35–40. https://doi.org/10.1115/1.3261876.
[9] V. Wikström, E. Höglund, R. Larsson, Wear of bearing liners at low speed rotation of shafts with contaminated oil, Wear. 162–164 (1993) 996–1001. https://doi.org/10.1016/0043-1648(93)90110-8.
[10] K. Mizuhara, M. Tomimoto, T. Yamamoto, Effect of particles on lubricated friction, Tribol. Trans. 43 (2000) 51–56. https://doi.org/10.1080/10402000008982312.
[11] J.K. Duchowski, K.G. Collins, W.M. Dmochowski, Experimental evaluation of filtration requirements for journal bearings operating under different contaminant levels, Lubr. Eng. 58 (2002) 34–39.
[12] M. Tomimoto, K. Mizuhara, T. Yamamoto, Effect of particles on lubricated friction - Theoretical analysis of friction caused by particles in journal bearing, S.A.E. Trans. 45 (2002) 47–54. https://doi.org/10.1080/10402000208982520.
[13] M.M. Khonsari, S.H. Wang, On the role of particulate contamination in scuffing failure, Wear. 137 (1990) 51–62. https://doi.org/10.1016/0043-1648(90)90017-5.
[14] M.M. Khonsari, M.D. Pascovici, B.V. ny Kucinschi, On the Scuffing Failure of Hydrodynamic Bearings in the Presence of an Abrasive Contaminant, 1 (1999) 90–96. https://doi.org/https://doi.org/10.1115/1.2833816.
[15] M.D. Pascovici, M.M. Khonsari, Scuffing failure of hydrodynamic bearings due to an abrasive contaminant partially penetrated in the bearing over-layer, J. Tribol. 123 (2001) 430–433. https://doi.org/10.1115/1.1329877.
[16] B. Bou-Said, H. Boucherit, M. Lahmar, On the influence of particle concentration in a lubricant and its rheological properties on the bearing behavior, Mech. Ind. 13 (2012) 111–121. https://doi.org/10.1051/meca/2012006.
[17] H. Boucherit, B. Bou-Saïd, M. Lahmar, The effect of solid particle lubricant contamination on the dynamic behavior of compliant journal bearings, Lubr. Sci. 29 (2017) 425–439. https://doi.org/10.1002/ls.1378.
[18] M.M. Khonsari, E.R. Booser, Effect of contamination on the performance of hydrodynamic bearings, Proc. Inst. Mech. Eng. Part J J. Eng. Tribol. 220 (2006) 419–428. https://doi.org/10.1243/13506501J00705.
[19] J.K. Duchowski, Examination of journal bearing filtration requirements, Lubr. Eng. 54 (1998) 18–28.
[20] A. Dadouche, M.J. Conlon, Operational performance of textured journal bearings lubricated with a contaminated fluid, Tribol. Int. 93 (2016) 377–389. https://doi.org/10.1016/j.triboint.2015.09.022.
[21] J. Sep, A. Kucaba-Pi, Experimental testing of journal bearings with two-component surface layer in the presence of an oil abrasive contaminant, Wear. 249 (2001) 1090–1095. https://doi.org/10.1016/S0043-1648(01)00848-1.
[22] J. Sep, L. Tomczewski, L. Galda, A. Dzierwa, The study on abrasive wear of grooved journal bearings, Wear. 376–377 (2017) 54–62. https://doi.org/10.1016/j.wear.2017.02.034.
[23] J. Sep, L. Galda, R. Oliwa, K. Dudek, Surface layer analysis of helical grooved journal bearings after abrasive tests, Wear. 448–449 (2020) 203233. https://doi.org/10.1016/j.wear.2020.203233.

[24] B. Vengudusamy, M. Von Hoersten, M. Schweigkofler, M. Kuhn, W. Litwin, Hydro lubricants: water-based lubricants for hydropower applications, in: Proc. HYDRO 2018, 15-17 October, Gdańsk, Pol., Gdańsk, 2018: pp. 1–7.

[25] W. Litwin, A. Olszewski, Assessment of possible application of water-lubricated sintered brass slide bearing for marine propeller shaft. 2012 | POLISH MARITIME RESEARCH 19 (4) , pp.54-61 https://doi.org/10.2478/v10012-012-0040-4

[26] W. Litwin, Water lubricated marine stern tube bearings - attempt at estimating hydrodynamic capacity, ASME/STLE International Joint Tribology Conference. 2010. Proceedings of the ASME/STLE International Joint Tribology Conference - 2009

[27] M. Damrat, A. Zaborska, M. Zajaczkowski, Sedimentation from suspension and sediment accumulation rate in the River Vistula prodelta, Gulf of Gdańsk (Baltic Sea), Oceanologia. 55 (2013) 937–950. https://doi.org/10.5697/oc.55-4.937.

[28] T. Leipe, F.X. Gingele, The kaolinite/chlorite clay mineral ratio in surface sediments of the southern Baltic Sea as an indicator for long distance transport of fine-grained material, Baltica. 16 (2003) 31–37.

[29] C.L. Dong, C.Q. Yuan, X.Q. Bai, Y. Yang, X.P. Yan, Study on wear behaviours for NBR/stainless steel under sand water-lubricated conditions, Wear. 332–333 (2015) 1012–1020. https://doi.org/10.1016/j.wear.2015.01.009.

[30] R. Orndorff, Water lubricated rubber bearings, history and new developments, Nav Eng J. (1985) 39–52.

[31] A. Barszczewska, Experimental Research on Insufficient Water Lubrication of Marine Stern Tube Journal Bearing with Elastic Polymer Bush, Polish Marit. Res. 27 (2020) 91–102. https://doi.org/10.2478/pomr-2020-0069.

[32] DNVGL-CP-0081. Synthetic bearing bushing materials, 2016.

[33] C. Yuan, Z. Guo, W. Tao, C. Dong, X. Bai, Effects of different grain sized sands on wear behaviours of NBR/casting copper alloys, Wear. 384–385 (2017) 185–191. https://doi.org/10.1016/j.wear.2017.02.019.

[34] C. Yang, X. Zhou, J. Huang, F. Kuang, X. Liu, Effects of sediment size and type on the tribological properties of NBR in water, Wear. 477 (2021) 203800. https://doi.org/10.1016/j.wear.2021.203800.

[35] R. Gheisari, A.A. Polycarpou, Three-body abrasive wear of hard coatings: Effects of hardness and roughness, Thin Solid Films. 666 (2018) 66–75. https://doi.org/10.1016/j.tsf.2018.07.052.

[36] R. Gheisari, A.A. Polycarpou, Tribological performance of graphite-filled polyimide and PTFE composites in oil-lubricated three-body abrasive conditions, Wear. 436–437 (2019) 203044. https://doi.org/10.1016/j.wear.2019.203044.

[37] M. Xue Shen, B. Li, S. Li, G. Yao Xiong, D. hui Ji, Z. nan Zhang, Effect of particle concentration on the tribological properties of NBR sealing pairs under contaminated water lubrication conditions, Wear. 456–457 (2020) 203381. https://doi.org/10.1016/j.wear.2020.203381.

[38] R. Prehn, F. Haupert, K. Friedrich, Sliding wear performance of polymer composites under abrasive and water lubricated conditions for pump applications, Wear. 259 (2005) 693–696. https://doi.org/10.1016/j.wear.2005.02.054.

[39] Z. Jia, Z. Guo, C. Yuan, Effect of Material Hardness on Water Lubrication Performance of Thermoplastic Polyurethane under Sediment Environment, J. Mater. Eng. Perform. 30 (2021) 7532–7541. https://doi.org/10.1007/s11665-021-05912-z.

[40] A. Barszczewska, E. Piatkowska, W. Litwin, Selected Problems of Experimental Testing Marine Stern Tube Bearings, Polish Marit. Res. 26 (2019) 142–154. https://doi.org/10.2478/pomr-2019-0034.

[41] E. Piątkowska, Influence of solid particle contamination on the wear process in water lubricated marine strut bearings with NBR and PTFE bushes, Polish Marit. Res. 112 (2022) 167–178. https://doi.org/10.2478/pomr-2021-0059.